A MODEL FOR STEADY-STATE, BALLISTIC CHARGE TRANSPORT THROUGH QUANTUM DOT LAYER SUPERLATTICES

MANOJ RAJAGOPALAN† AND PINAKI MAZUMDER †

Abstract. We derive a model for one-dimensional charge-transport through two-terminal semiconducture heterostructure nano-devices comprising stacked layers of quantum dots with transverse Bravais lattice layout. All dots in a layer are assumed to be identical. The stacked layers are assumed to be perfectly vertically-aligned so that the entire device has a well-defined transverse unit-cell. We allow for an arbitrary sequence of quantum dot layers and intervening spacer and wetting layers between two heavily-doped, ohmic contacts. The model naturally accounts for long-range, inter-dot correlations. We rigorously prove that the device behaves as a diffraction grating which distributes incident wavefunction-phases into specific patterns of transmitted phases. This establishes several mathematical properties that allow efficient decomposition of the problem and permit feasible strategies for computational implementation. We motivate the study of this family of devices citing experimental developments.

Key words. quantum dot superlattices, mesoscopic charge transport

AMS subject classifications. 81Q80, 81Q05, 34L10, 34L25, 34A05, 46F25, 35Q40, 35C99

1. Introduction.

Advances in *fabrication* technology have shown that layers of quantum dots can be grown in regular layouts with only small variations in dot geometry over the extent of a layer [36, 23, 28]. Diverse possibilities exist for the size, shape [38, 15, 20, 39, 21, 24], dot-density [30] and material system - III-V (principally InAs/GaAs), Group IV [11], II-VI [18], and IV-VI [33] - with quasi-periodic layouts [29]. Also, vertically-stacked layers tend to align with long-range, three-dimensional order [8] resulting in lattices with simple cube [19, 33] and FCC unit-cells [33]. This is reminiscent of the atomic arrangement in intrinsic semiconductor material crystals which is the foundation for many of their interesting properties. Because quantum dots are artificial atoms, analogy suggests that stacked quantum dot layers (SQDL) may also possess interesting electronic and optical properties that could give rise to a promising family of devices and applications.

Interesting open-system, electronic devices like resonant tunneling diodes have been demonstrated using SQDL [31]. Since the experimental demonstration of quantum-mechanical tunneling by Chang *et. al.* [9], many semiconductor nano-heterostructure electronic devices have been proposed which exhibit non-monotonic current-voltage (I-V) characteristics. Proof-of-concept circuits based on idealizations of negative differential resistance in the I-V characteristics of *conventional* resonant tunneling diodes [35], built epitaxially with alternating layers of lattice-matched material films, indicate the potential of heterostructure devices in realizing new and existing applications with superior speed and power performance [25]. The use of lattice-mismatched materials in epitaxial growth leads to pseudomorphic-strain-induced quantum dot formation [12]. Their self-assembly with long-range order invites questions on the characteristics of charge transport obtainable from this class of materials, and motivates the advancement of models beyond existing ones.

The large space of parameters - size, shape, density, material-system, layout, stacking - that affect device characteristics makes modeling and simulation indis-

†Dept. of Electrical Engineering and Computer Science, University of Michigan, Ann Arbor, MI 48109, USA ({rmanoj, mazum} @eecs.umich.edu)

pensable aids to experiment. If process-technology matures to permit the growth of nano-voids [22] and antidots [14] in regular geometries, then quantum-dot composition would add an extra dimension to the parameter-space. Three-dimensional modeling is necessary for these device-geometries and naive models rapidly grow to exhaust resources provided by powerful computers even at modest problem-sizes. Atomistic modeling is a possibility but the complexity and resource pressure are in general high and are expected to be compounded by the inclusion of long-range inter-dot correlations that are characteristic of these systems.

The envelope-function approach [2, 3] has had reasonable success in predicting charge-transport characteristics of simple heterostructure devices. We therefore propose an envelope-function-based model for steady-state, one-dimensional charge-transport through SQDL along the growth-direction. In doing so, we establish many mathematical properties of SQDL systems that allow highly parallel implementation with low pressure on computational resources. A semi-empirical extension of this model could serve as a bridge between expensive, physically-accurate atomistic models and simple, phenomenological, behavioral models. This model will also allow estimation of the lower time- and resource-bounds for simulating SQDL systems. Lastly, the beauty of the fabricated structures and the challenges in mathematical modeling and computational complexity make the development of such a model an interesting problem.

Most theoretical and experimental investigations (e.g. [6, and references therein]) study electronic structure and optical response of isolated dots - relatively few address the problem of charge-transport especially through an open, extended system of quantum dots. Ko and Inkson [17] propose the use of the scattering-matrix, or S-matrix, structure for resonant tunneling through multilayer systems. Xu [37] applies the S-matrix approach to study transport through 1D periodic arrays of antidots in a 2D electron-gas (2D) in a manner similar to this work. Mizuta *et. al.* [27] study transport through lithographically-etched, free-standing, isolated quantum dots using the S-matrix method.

Section 2 describes the problem, notation and conventions. Section 3 presents the general formalism and the dependence of the current on the carrier wavefunction when the device is driven by an externally-applied voltage. Sections 4 and 5 develop the method for wavefunction calculation, derive various special properties and simplifications arising from the lateral translational symmetry, and prove that incident wavefunction phases exhibit specific patterns of diffraction when eventually transmitted. Section 6 extends the general formalism of Section 3 with these results and completes the model with a formula for total current per lateral-unit-cell. Section 7 concludes with a summary, critique and mention of future work. For brevity, each of these sections includes only the important results - various appendices furnish the details.

2. Conventions, terminology, and notation . In this section, we standardize most of the notation, terminology, and conventions occurring throughout this work. A few other definitions are made in relevant contexts when their scope is local.

Except for Airy functions, the prime symbol ($\prime$) *does not* denote differentiation.

2.1. Device description . The device is grown along the $z-$axis. Fig. 2.1 depicts the structure of devices considered in this work. Two ohmic contacts enclose an arbitrary sequence of regions that are either spacers or QDL. Spacers are uniform regions of a single, isotropic material. The QDL are regions where the effective-mass and/or potential energy profile show variation. This includes the matrix of high bandgap material surrounding the islands of lower bandgap material. Within each QDL all quantum dots are identical and grow in a perfect, two-dimensional $(x-y)$ Bravais lattice layout - therefore effective-mass and potential energy lateral variation is periodic. There can be more than one dot per unit-cell. All QDL are vertically aligned - the positions and orientations of their unit-cells are exactly-matched so that the entire has a well-defined lateral Bravais lattice structure and unit-cell. The QDL may or may not have wetting layers depending on their growth mode. We assume uniform strain and potential energy distribution in the wetting layers and relegate any (periodic) non-uniformities to the QDL. Therefore, wetting layers are also grouped with spacers. Voltage bias is applied along the growth (z) direction and does not distort the structure of the device. We assume the device to be of infinite lateral extent, i.e., we ignore fringe effects from actual finite extents. We use $N_{\|}$ to symbolically denote the (infinite) number of lateral unit-cells in the device.

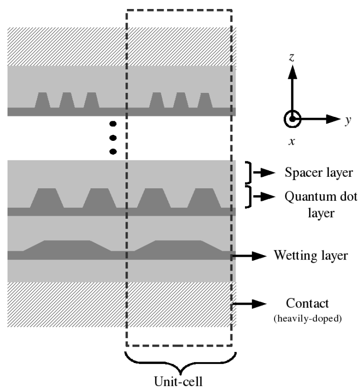

FIGURE 2.1. *Schematic depiction of the stacked quantum dot layer device*

The (relative) effective-mass and potential energy spatial distributions, along with doping and temperature information at the contacts, completely specify the problem in the mathematical sense. We use $m(\mathbf{r})$ to denote *relative* effective-mass function in the device, and $\mu(\mathbf{r})$ to denote its reciprocal - various superscripts and subscripts may qualify the relevant region or interface. We use $V(r)$ to denote the spatial variation of the *envelope* of the true potential energy experienced by a carrier particle, and E to denote is total energy.

2.2. Representation of functions and operators. We follow the bra-ket notation of Dirac and consider functions and operators to be vectors and matrices, respectively, in infinite-dimensional function-space - for a brief yet excellent introduction we refer the reader to Chapter 1 of [32]. This allows simple notation regardless of dimension.

We use $\mathbf{I}$ to denote the identity operator or its matrix. We use $\mathbf{0}$ to denote the zero matrix. The dimensions of these quantities are implicit in the context.

Real-space coordinates are denoted using *lateral* coordinates $\mathbf{r}_{\|} \overset{\text{def}}{=} (x, y) \in \mathbb{R}^2$ and *longitudinal* coordinates $z \in \mathbb{R}$. We deal mostly with functions of $\mathbf{r}_{\|}$ at various values of z. Functions $f(\mathbf{r})$ of the three spatial variables are represented as $f\left(\mathbf{r}_{\|}, z\right)$ and the 2D restriction of $f(\mathbf{r})$ to a fixed value of z is denoted $f\left(\mathbf{r}_{\|}; z\right)$. In general, a function g of variables $\mathbf{x}$ with parametric dependence on variables $\mathbf{c}$ is denoted $g(\mathbf{x}; \mathbf{c})$.

We use $\mathbf{0}_{\|}$ to denote $(0,0) \in \mathbb{R}^2$.

Let $\mathbb{F} \stackrel{\text{def}}{=} \left\{ f \mid f : \mathbb{R}^2 \to \mathbb{C} \,,\, \iint_{\mathbb{R}^2} |f|^2 \, d^2 r_\parallel < \infty \right\}$ denote the set of complex-valued, square-integrable, functions of $\mathbf{r}_\parallel$. Since $\iint_{\mathbb{R}^2} \left| \Psi \left(\mathbf{r}_\parallel ; z \right) \right|^2 \, d^2 r_\parallel$ must be bounded for any wavefunction Ψ, all wavefunctions belong to this set. Each $\mathbf{r}_\parallel \in \mathbb{R}^2$ corresponds uniquely with the element (ket) $\left| \mathbf{r}_\parallel \right\rangle \in \mathbb{R} \otimes \mathbb{R}$, and each $f \in \mathbb{F}$ corresponds uniquely with the map $|\mathbf{f}\rangle : \mathbb{R} \otimes \mathbb{R} \to \mathbb{C}$ such that $\left| \mathbf{r}_\parallel \right\rangle \stackrel{|\mathbf{f}\rangle}{\mapsto} f \left(\mathbf{r}_\parallel \right)$. We use the term *function* to refer to f or $|\mathbf{f}\rangle$. The set $\mathcal{F} \stackrel{\text{def}}{=} \{ |\mathbf{f}\rangle \mid f \in \mathbb{F} \}$ forms a Hilbert space over the field of complex numbers $\mathbb{C}$ with basis $\left\{ \left| \mathbf{r}_\parallel \right\rangle \mid \mathbf{r}_\parallel \in \mathbb{R}^2 \right\} \equiv \mathbb{R} \otimes \mathbb{R}$, that is orthonormal, $\forall \mathbf{r}_{\parallel 1}, \mathbf{r}_{\parallel 2} \in \mathbb{R}^2 : \left\langle \mathbf{r}_{\parallel 1} \mid \mathbf{r}_{\parallel 2} \right\rangle = \delta \left(\mathbf{r}_{\parallel 1} - \mathbf{r}_{\parallel 2} \right)$ (Dirac delta function), and complete, $\sum_{\mathbf{r}_\parallel \in \mathbb{R}^2} \left| \mathbf{r}_\parallel \right\rangle \left\langle \mathbf{r}_\parallel \right| = \mathbf{I}$. The inner-product for this space is $\forall f_1, f_2 \in \mathcal{F} : \langle \mathbf{f}_1 \mid \mathbf{f}_2 \rangle \stackrel{\text{def}}{=} \iint_{\mathbb{R}^2} f_1^* \left(\mathbf{r}_\parallel \right) f_2 \left(\mathbf{r}_\parallel \right) d^2 r_\parallel$. For any $\mathbf{r}_\parallel \in \mathbb{R}^2$, $f \left(\mathbf{r}_\parallel \right) \equiv \left\langle \mathbf{r}_\parallel \mid \mathbf{f} \right\rangle$ is the coordinate of $|\mathbf{f}\rangle$ along basis-element $\left| \mathbf{r}_\parallel \right\rangle$ in the *real-space representation* of $|\mathbf{f}\rangle$.

In specific contexts, we extend this ket-notation to functions of 1 and 3 spatial variables.

We use $\mathbb{K}$ to denote the set of 2D wavevectors $\mathbf{k}_\parallel \in \mathbb{R}^2$. The family of all normalized, 2D planewaves, $\mathcal{K} \stackrel{\text{def}}{=} \left\{ \left| \mathbf{k}_\parallel \right\rangle \mid \mathbf{k}_\parallel \in \mathbb{K}, \left\langle \mathbf{r}_\parallel \mid \mathbf{k}_\parallel \right\rangle = \frac{1}{2\pi} e^{i \mathbf{k}_\parallel \bullet \mathbf{r}_\parallel} \right\}$, $\mathbf{r}_\parallel \in \mathbb{R}^2$, also forms a complete, orthonormal basis (termed the *reciprocal-space basis*) for $\mathcal{F}$, i.e., $\forall \mathbf{k}_{\parallel 1}, \mathbf{k}_{\parallel 2} \in \mathbb{K}$, $\left\langle \mathbf{k}_{\parallel 1} \mid \mathbf{k}_{\parallel 2} \right\rangle = \delta \left(\mathbf{k}_{\parallel 1} - \mathbf{k}_{\parallel 2} \right)$ and $\sum_{\mathbf{k}_\parallel \in \mathbb{K}} \left| \mathbf{k}_\parallel \right\rangle \left\langle \mathbf{k}_\parallel \right| = \mathbf{I}$. The *reciprocal-space representation* of a function $|\mathbf{f}\rangle$ in this basis is defined by coordinates $\hat{f} \left(\mathbf{k}_\parallel \right) \stackrel{\text{def}}{=} \left\langle \mathbf{k}_\parallel \mid \mathbf{f} \right\rangle$ and is related to its real-space representation through unitary, change-of-basis transformations - the 2D Fourier transform and its inverse,

$$\hat{f} \left(\mathbf{k}_\parallel \right) = \left\langle \mathbf{k}_\parallel \mid \mathbf{f} \right\rangle = \mathfrak{F}_\parallel \left[f \left(\mathbf{r}_\parallel \right) \right] \left(\mathbf{k}_\parallel \right) \stackrel{\text{def}}{=} \frac{1}{2\pi} \iint_{\mathbb{R}^2} e^{-i \mathbf{k}_\parallel \bullet \mathbf{r}_\parallel} f \left(\mathbf{r}_\parallel \right) d^2 r_\parallel, \tag{2.1}$$

$$f \left(\mathbf{r}_\parallel \right) = \left\langle \mathbf{r}_\parallel \mid \mathbf{f} \right\rangle = \mathfrak{F}_\parallel^{-1} \left[\hat{f} \left(\mathbf{k}_\parallel \right) \right] \left(\mathbf{r}_\parallel \right) \stackrel{\text{def}}{=} \frac{1}{2\pi} \iint_{\mathbb{K}} \hat{f} \left(\mathbf{k}_\parallel \right) e^{i \mathbf{k}_\parallel \bullet \mathbf{r}_\parallel} d^2 k_\parallel. \tag{2.2}$$

Vectors are denoted using bold-face, small, roman or greek letters. Operator and matrices are represented using bold-face, capital, roman letters. We use $\mathbf{M}(z)$ to denote the relative-effective-mass operator at a fixed value of z. It has diagonal-matrix real-space representation, $\left\langle \mathbf{r}_\parallel \right| \mathbf{M} (z) \left| \mathbf{r'}_\parallel \right\rangle = m \left(\mathbf{r}_\parallel ; z \right) \delta \left(\mathbf{r}_\parallel = \mathbf{r'}_\parallel \right)$, and has the effect, $\left\langle \mathbf{r}_\parallel \right| \mathbf{M} \left| \mathbf{f} \right\rangle = m \left(\mathbf{r}_\parallel ; z \right) f \left(\mathbf{r}_\parallel \right)$. Its inverse is the reciprocal effective-mass operator $\left\langle \mathbf{r}_\parallel \right| \mathbf{M}^{-1} (z) \left| \mathbf{f} \right\rangle = \mu \left(\mathbf{r}_\parallel ; z \right) f \left(\mathbf{r}_\parallel \right) \equiv \frac{1}{m \left(\mathbf{r}_\parallel ; z \right)} f \left(\mathbf{r}_\parallel \right)$. It is useful in boundary-condition contexts.

2.3. Periodic functions, Fourier series, and Brillouin zone . We use $\mathbf{R}_{\parallel 1}$, $\mathbf{R}_{\parallel 2} \in \mathbb{R}^2$ to denote the primitive vectors of the lateral unit-cell $\mathbf{\Omega}_\parallel$. The unit-cell area is denoted by $\left| \Omega_\parallel \right| = \left| \mathbf{R}_{\parallel 1} \times \mathbf{R}_{\parallel 2} \right|$. Various lattice vectors are denoted by $\mathbf{R}_{\parallel lm} \stackrel{\text{def}}{=} l \mathbf{R}_{\parallel 1} + m \mathbf{R}_{\parallel 2}$, $(l, m) \in \mathbb{Z}^2$. The reciprocal-space primitive vectors $\mathbf{G}_{\parallel 1}$ and $\mathbf{G}_{\parallel 2}$, such that $\mathbf{R}_{\parallel i} \bullet \mathbf{G}_{\parallel j} = (2\pi)^2 \delta_{ij}$ (Kronecker delta function), define the extent of the first Brillouin zone, $\mho_\parallel$.

Periodic functions $u \left(\mathbf{r}_\parallel + \mathbf{R}_{\parallel lm} \right) \equiv u \left(\mathbf{r}_\parallel \right), \forall (l, m) \in \mathbb{Z}^2$, have Fourier series representations of the form [16],

$$u \left(\mathbf{r}_\parallel \right) = \sum_{(l,m) \in \mathbb{Z}^2} \hat{u}_{lm} e^{i \mathbf{G}_{\parallel lm} \bullet \mathbf{r}_\parallel}, \quad \hat{u}_{lm} = \frac{1}{\left| \Omega_\parallel \right|} \iint_{\Omega_\parallel} e^{-i \mathbf{G}_{\parallel lm} \bullet \mathbf{r}_\parallel} u \left(\mathbf{r}_\parallel \right) d^2 r_\parallel, \tag{2.3}$$

where $\mathbf{G}_{\parallel lm} \stackrel{\text{def}}{=} l \mathbf{G}_{\parallel 1} + m \mathbf{G}_{\parallel 2}$, $(l, m) \in \mathbb{Z}^2$ denote various reciprocal-lattice vectors and comprise the set $\mathbb{G} \stackrel{\text{def}}{=} \left\{ \mathbf{G}_{\parallel lm} \mid (l, m) \in \mathbb{Z}^2 \right\}$.

The Fourier-series coefficients, $\hat{u}_{lm}$, are collectively represented as a countably-infinite-dimensional vector $\hat{\mathbf{u}}$. The Fourier-series coefficients of the product of two periodic functions $u\left(\mathbf{r}_\|\right)$ and $v\left(\mathbf{r}_\|\right)$ are represented by $\widehat{(uv)}_{lm}$, $(l,m) \in \mathbb{Z}^2$, and can be calculated from convolution $\widehat{(uv)}_{lm} \equiv (\hat{\mathbf{u}} \odot \hat{\mathbf{v}})_{lm} \stackrel{\text{def}}{=} \sum_{(l',m')\in\mathbb{Z}^2} \hat{u}_{l'm'}\hat{v}_{(l-l')(m-m')}$. We use the dot-product notation to represent the sum of products of like components of vectors, $\mathbf{a} \bullet \mathbf{b} = \sum_i a_i b_i$ where i is an index variable that iterates across appropriate limits and the summation is understood to represent integration when the domain of i is continuous. If $u\left(\mathbf{r}_\|\right)$ and $v\left(\mathbf{r}_\|\right)$ are real-valued, then $\hat{u}_{-(lm)} \equiv \hat{u}^*_{lm}$, $\hat{v}_{-(lm)} \equiv \hat{v}^*_{lm}$ and therefore, $\widehat{(uv)}_{00} \equiv (\hat{\mathbf{u}} \odot \hat{\mathbf{v}})_{00} = \sum_{(l,m)\in\mathbb{Z}^2} \hat{u}_{lm}\hat{v}_{-lm} \equiv \hat{\mathbf{u}} \bullet \hat{\mathbf{v}}^* \equiv \hat{\mathbf{u}}^* \bullet \hat{\mathbf{v}}$. This equivalence is frequently used.

We use $\mathbf{g}_\|$ to denote vectors within the Brillouin zone, i.e.,

$$\mho_\| \stackrel{\text{def}}{=} \left\{ \mathbf{g}_\| \,|\, \mathbf{g}_\| = x\mathbf{G}_{\|1} + y\mathbf{G}_{\|2},\ x, y \in [-\frac{1}{2}, \frac{1}{2}) \right\}.$$

We use $\mathbf{g}_{\|lm} \stackrel{\text{def}}{=} \mathbf{g}_\| + \mathbf{G}_{\|lm}$, $(l,m) \in \mathbb{Z}^2$ to denote displacements of $\mathbf{g}_\|$ by reciprocal lattice vectors, and $\mathbb{G}_{\left[\mathbf{g}_\|\right]} \stackrel{\text{def}}{=} \left\{\mathbf{g}_{\|lm} \mid (l,m) \in \mathbb{Z}^2\right\}$ to denote the full family of such displacements. Therefore $\mathbb{G} \equiv \mathbb{G}_{\left[\mathbf{0}_\|\right]}$.

2.4. Indices, basis-sets, and spanning-spaces. Real- and reciprocal-space vectors, $\mathbf{r}_\| \in \mathbb{R}^2$ and $\mathbf{k}_\| \in \mathbb{K}$, serve as indices to elements in basis-sets $\mathbb{R} \otimes \mathbb{R}$ and $\mathcal{K}$, respectively, for $\mathcal{F}$. We employ calligraphic symbols to denote (sub)sets of basis kets for the corresponding (sub)sets of reciprocal-space vectors, $\mathcal{K} \stackrel{\text{def}}{=} \left\{\left|\mathbf{k}_\|\right\rangle \mid \mathbf{k}_\| \in \mathbb{K}\right\}$,$\mathcal{G} \stackrel{\text{def}}{=} \left\{\left|\mathbf{G}_{\|lm}\right\rangle \mid \mathbf{G}_{\|lm} \in \mathbb{G}\right\}$ and $\mathcal{G}_{\left[\mathbf{g}_\|\right]} \stackrel{\text{def}}{=} \left\{\left|\mathbf{g}_{\|lm}\right\rangle \mid \mathbf{g}_{\|lm} \in \mathbb{G}_{\left[\mathbf{g}_\|\right]}\right\}$. We use the following notation for (sub)spaces spanned by these basis-element sets, $\mathcal{F} = \operatorname{span}\mathcal{K}$, $\mathcal{F}_{\left[\mathbf{g}_\|\right]} \stackrel{\text{def}}{=} \operatorname{span}\mathcal{G}_{\left[\mathbf{g}_\|\right]}$.

Because the entire device possesses a well-defined lateral crystal structure, homogeneous regions like spacers and contacts can also be tiled into an identical Bravais lattice comprised of homogeneous unit-cells. The following definitions are useful in reconciling the behavior of the wavefunction across homogeneous regions and the QDL.

Definition 2.1. *For each $\mathbf{k}_\| \in \mathbb{K}$, the corresponding* $\mathbf{k}_\|$-subspace *of $\mathcal{F}$ is the one-dimensional subspace $\mathcal{F}_{\mathbf{k}_\|}$ spanned by planewave basis element $\left|\mathbf{k}_\|\right\rangle$. Therefore, $\mathcal{F}_{\mathbf{k}_\|} \stackrel{def}{=} span\left\{\left|\mathbf{k}_\|\right\rangle\right\}$.*

Definition 2.2. *For each $\mathbf{g}_\| \in \mho_\|$, the Brillouin-zone-vector subspace, or* BZV-subspace, *is defined as $\mathcal{F}_{\left[\mathbf{g}_\|\right]} \stackrel{def}{=} span\,\mathcal{G}_{\left[\mathbf{g}_\|\right]} = span\left\{\left|\mathbf{g}_{\|lm}\right\rangle \mid (l,m) \in \mathbb{Z}^2\right\}$. It is the subspace of $\mathcal{F}$ spanned by the countably-infinite set of kets comprising the equivalence-class of $\mathbf{g}_\|$. Also, $\mathcal{F}_{\left[\mathbf{g}_\|\right]} = \bigoplus_{(l,m)\in\mathbb{Z}^2} \mathcal{F}_{\mathbf{g}_{\|lm}}$.*

Definition 2.3. *A* natural order *of the basis elements $\mathbb{K}$ is the partially-ordered set $\mathbb{K}^{\leq}$ obtained by imposing a partial order $\leq$ on $\mathbb{K}$, defined such that*

$$\forall \mathbf{g}_\|, \mathbf{g'}_\| \in \mho_\|,\ \forall l, l', m, m' \in \mathbb{Z} : \mathbf{g}_{\|lm} \leq \mathbf{g'}_{\|l'm'} \qquad \textit{if} \qquad \mathbf{g}_\| < \mathbf{g'}_\|$$

for some total order $<$ imposed on $\mho_\|$. Appendix A presents preliminary facts based on the above definitions that will be frequently used throughout this work.

3. General formalism . As shown in Fig. 3.1, we assume that the total current-density through the device is the resultant from four constituent, undirectional sub-current-densities,

$$(3.1)\; J\left(V_{bias}\right) = J_{1\to 2,e}\left(V_{bias}\right) + J_{2\to 1,e}\left(V_{bias}\right) + J_{1\to 2,h}\left(V_{bias}\right) + J_{2\to 1,h}\left(V_{bias}\right),$$

where the subscripts of the form INJ $\to$ TRA, c refer to the transport of carrier type c (e for electrons, h for holes) from the injecting contact to the transmitting contact, and V_{bias} is the externally applied potential difference between the two contacts that drives transport. We assume ballistic transport of the charge carriers.

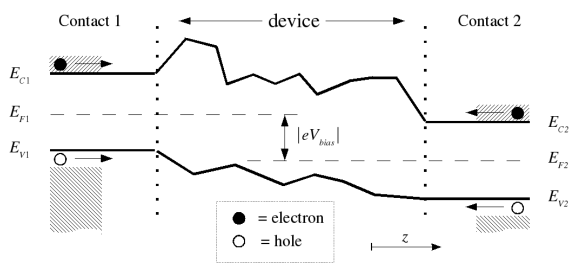

FIGURE 3.1. *Dominant contributions to net current-density for a two terminal device. The shading in the contact regions schematically depicts high electron density.*

We assume thermal equilibrium in the heavily-doped, ohmic contacts and that the supplied carrier states incident on the device are planewaves. We assume that each unidirectional sub-current is the weighted-accumulation of transmitted-probability-currents from *independent, elastic* scattering of all incident states incident at the corresponding injecting contact,

$$(3.2)\quad J_{\text{INJ}\to\text{TRA},c}\left(V_{bias}\right) = 2q_c \iint_{\mathbb{K}} \int_0^{\infty} N_c^{(\text{INJ})}\left(\mathbf{k}\right) f_c^{(\text{INJ})}\left(\mathbf{k}; V_{bias}\right) \left\langle v_{\text{INJ}\to\text{TRA},c}\left(\mathbf{k}; V_{bias}\right)\right\rangle dk_z d^2k_{\|},$$

where the $z-$axis is along INJ$\to$TRA (=1 $\to$ 2 or 2 $\to$ 1), $\mathbf{k} = \mathbf{k}_{\|} + k_z\hat{\mathbf{z}}$ is the wavevector for the incident planewave, q_c is the charge on a single carrier particle (e for holes,$-e$ for electrons), the factor of 2 accounts for both spins, and the general expressions for the density-of-states and the Fermi-Dirac distribution function at contact *CON* (=INJ or TRA) are [34],

$$(3.3)\qquad N_c^{(\text{CON})}\left(\mathbf{k}\right) = \frac{1}{\left(2\pi\right)^3}, \qquad f_c^{(\text{CON})}\left(\mathbf{k}\right) = \frac{1}{1+\exp\left(\frac{E(\mathbf{k})-E_{F,c}^{(\text{CON})}}{k_B T}\right)}$$

where $E\left(\mathbf{k}\right)$ is the dispersion relation, $E_{F,c}^{(\text{CON})}$ is the Fermi energy which depends on doping, and T is the temperature. The average z-velocity is obtained from the expression for the spatial average of the transmitted, local probability-current,

$$(3.4)\quad j_{\text{INJ}\to\text{TRA},c}\left(\mathbf{r}_{\|}; \mathbf{k}, V_{bias}\right) \stackrel{\text{def}}{=} \frac{\hbar}{m_c^{(\text{TRA})}} \text{Im}\left[\Psi_c^{(\text{TRA})*}\left(\mathbf{r}_{\|}, z; \mathbf{k}, V_{bias}\right) \frac{\partial}{\partial z}\Psi_c^{(\text{TRA})}\left(\mathbf{r}_{\|}, z; \mathbf{k}, V_{bias}\right)\right]\Bigg|_{z\geq L}$$

$$\text{(3.5)}\qquad \left\langle v_{\text{INJ}\to\text{TRA},c}\left(\mathbf{k};V_{bias}\right)\right\rangle = \frac{1}{N_{\|}\Omega_{\|}}\iint_{\mathbb{R}^2} j_{\text{INJ}\to\text{TRA},c}\left(\mathbf{r}_{\|};\mathbf{k},V_{bias}\right) d^2 r_{\|},$$

where $m_c^{(\text{TRA})}$ is the carrier-particle mass in the transmitting contact, L is the length of the device, and $\Psi_c^{(\text{TRA})}$ is its scattered wavefunction.

The wavefunction is calculated over the entire device by solving the time- independent Schrödinger equation (TISE) with boundary conditions supplied by the form of the wavefunctions at both contacts. We assume that the contacts are isotropic and uniform with flat band-profiles despite the applied bias (even in self-consistent co-solution with the Poisson equation, this assumption must be made deep enough into the contact region), and that the dispersion relations are parabolic,

$$\text{(3.6)}\qquad E^{(\text{CON})}\left(\mathbf{k}\right) = \frac{\hbar^2 k^2}{2m_c^{(\text{CON})}} + V^{(\text{CON})},$$

where $V^{(\text{CON})}$ is the potential energy at the relevant contact due to applied voltage. Hence, for an incident state with wavevector $\mathbf{k}^{(\text{INC})} \stackrel{\text{def}}{=} \mathbf{k}_{\|}^{(\text{INC})} + k_z^{(\text{INC})}\hat{\mathbf{z}}$, and energy $E = E^{(\text{INJ})}\left(\mathbf{k}^{(\text{INC})};V_{bias}\right)$,

$$\begin{aligned}
&\text{(3.7)} & \Psi_c^{(\text{INJ})}\left(\mathbf{r};\mathbf{k}^{(\text{INC})}\right) &= \Psi_c^{(\text{INC})}\left(\mathbf{r};\mathbf{k}^{(\text{INC})}\right) + \Psi_c^{(\text{REFL})}\left(\mathbf{r};\mathbf{k}^{(\text{INC})}\right),\\
&\text{(3.8)} & \Psi_c^{(\text{INC})}\left(\mathbf{r};\mathbf{k}^{(\text{INC})}\right) &\stackrel{\text{def}}{=} e^{i\mathbf{k}\bullet\mathbf{r}},\\
&\text{(3.9)} & \Psi_c^{(\text{REFL})}\left(\mathbf{r};\mathbf{k}^{(\text{INC})}\right) &\stackrel{\text{def}}{=} \iint_{\mathbb{K}^{(\text{INJ})}(E)} \rho\left(\mathbf{k}^{(\text{INC})},\mathbf{k}\right) e^{i\mathbf{k}\bullet\mathbf{r}}\, d^2k,\\
&\text{(3.10)} & \Psi_c^{(\text{TRA})}\left(\mathbf{r};\mathbf{k}^{(\text{INC})}\right) &\stackrel{\text{def}}{=} \iint_{\mathbb{K}^{(\text{TRA})}(E)} \tau\left(\mathbf{k}^{(\text{INC})},\mathbf{k}\right) e^{i\mathbf{k}\bullet\mathbf{r}}\, d^2k,
\end{aligned}$$

$$\begin{aligned}
&\text{(3.11)} & \mathbb{K}^{(\text{INJ})}\left(E\right) &\stackrel{\text{def}}{=} \left\{\mathbf{k}\in\mathbb{R}^3 \,|\, E^{(\text{INJ})}\left(\mathbf{k}\right) = E,\ \mathbf{k}\bullet\hat{\mathbf{z}}\in\mathbb{R}^+\right\}\\
&\text{(3.12)} & &= \left\{\mathbf{k}_{\|} + k_z^{(\text{INJ})}\left(E,\mathbf{k}_{\|}\right)\hat{\mathbf{z}} \,|\, \mathbf{k}_{\|}\in\mathbb{K}_{\|}^{(\text{INJ})}\left(E\right)\right\},\\
&\text{(3.13)} & \mathbb{K}_{\|}^{(\text{INJ})}\left(E\right) &\stackrel{\text{def}}{=} \left\{\mathbf{k}_{\|}\in\mathbb{K} \,|\, E^{(\text{INJ})}\left(\mathbf{k}_{\|}\right) < E\right\},\\
&\text{(3.14)} & k_z^{(\text{CON})}\left(E,\mathbf{k}_{\|}\right) &= \left|\sqrt{\frac{2m_c^{(\text{CON})}}{\hbar^2}\left(E - V^{(\text{CON})}\right) - k_{\|}^2}\,\right|,\\
&\text{(3.15)} & \mathbb{K}^{(\text{TRA})}\left(E\right) &\stackrel{\text{def}}{=} \left\{\mathbf{k}\in\mathbb{R}^3 \,|\, E^{(\text{TRA})}\left(\mathbf{k}\right) = E,\ \mathbf{k}\bullet\hat{\mathbf{z}}\in\mathbb{R}^-\right\}\\
&\text{(3.16)} & &= \left\{\mathbf{k}_{\|} - k_z^{(\text{TRA})}\left(E,\mathbf{k}_{\|}\right)\hat{\mathbf{z}} \,|\, \mathbf{k}_{\|}\in\mathbb{K}_{\|}^{(\text{TRA})}\left(E\right)\right\},\\
&\text{(3.17)} & \mathbb{K}_{\|}^{(\text{TRA})}\left(E\right) &\stackrel{\text{def}}{=} \left\{\mathbf{k}_{\|}\in\mathbb{K} \,|\, E^{(\text{CON})}\left(\mathbf{k}_{\|}\right) < E\right\}.
\end{aligned}$$

The incident wavefunction is partially reflected into a distribution of states propagating along the $-z$ direction, and the superposition of both is the steady-state injecting-contact wavefunction. The contacts are assumed reflectionless and therefore, the injected wavefunction is elastically scattered into a distribution of states propagating along the $+z$ direction at the transmitting contact. We term $\rho\left(\mathbf{k},\mathbf{k}'\right)$ as the *bidirectional reflectance distribution function* (BRDF) and $\tau(\mathbf{k}, \mathbf{k}')$ as the *bidirectional transmittance distribution function* (BTDF), respectively, for probability amplitudes. In both cases, the distribution is over the iso-energy surface of wavevectors corresponding to the incident energy.

The envelope-function approach simplifies calculations by substituting the actual spatial potential energy distribution with its envelope, and substituting the true carrier mass with an effective-mass parameter that semi-empirically captures effects from rapid atomic-scale variations of the true potential energy, i.e., $m_c \mapsto m_{0c} m_c(\mathbf{r})$, where m_{0c} is the rest-mass of the carrier and $m_c(\mathbf{r})$ is its position-dependent, relative effective-mass. The solution to this new Schrödinger equation is the *envelope* of the true wavefunction, henceforth referred to as the envelope function or simply, the wavefunction. The expression for the transmitted-probability-current is the same as in Eqn. (3.4) with the effective-mass and envelope function replacing the true carrier mass and wavefunction.

By assuming the energy-reference to be the band minimum at the injecting contact, we may follow a unified formalism for each of the four unidirectional subcurrents.

$$V^{(\text{INJ})} \equiv 0, \qquad V^{(\text{TRA})} = \pm V_{bias} \tag{3.18}$$

We therefore drop symbols and subscripts pertinent to the bias voltage, carrier type, band, and transport direction in the following general procedure for solving the appropriate three-dimensional, single-band, effective-mass, time-independent Schrödinger equation (3D-SBEM-TISE) [10] for the 3D wavefunctions $|\Psi\rangle$ (neglecting relativistic effects and spin-orbit coupling),

$$[\mathbf{H}_{\text{KE}} + \mathbf{V}]\,|\Psi\rangle = E|\mathbf{\Psi}\rangle. \tag{3.19}$$

Here, E is the total energy of the particle, $\mathbf{V}$ is the operator corresponding to the potential-energy envelope, with $V(\mathbf{r}) \overset{\text{def}}{=} \langle \mathbf{r} \mid \mathbf{V} \rangle$ being the spatial envelope that includes effects from device-structure as well as externally-applied voltage (henceforth simply termed the potential energy function or PEF), and $\mathbf{H}_{\text{KE}}$ is the kinetic energy operator that includes the position-dependent effective-mass. Because of open boundary conditions, all $E \geq 0$ are allowed eigen-energies. We assume that the applied voltage drops entirely across the device in a linear manner.

Two frequently-used formulations for the kinetic energy component of the Hamiltonian are the BenDaniel-Duke form [5],

$$\begin{aligned} \langle \mathbf{r}|\, \mathbf{H}_{\text{KE}}^{(\text{BD})}\,|\Psi\rangle &\equiv \mathbf{H}_{\text{KE}}^{(\text{BD})}(\mathbf{r})\,\Psi(\mathbf{r}) \\ &\overset{\text{def}}{=} -\frac{\hbar^2}{2m_0}\nabla \bullet \left(\frac{1}{m(\mathbf{r})}\nabla\Psi(\mathbf{r})\right), \end{aligned} \tag{3.20}$$

and the form proposed by Bastard *et. al.* [4],

$$\begin{aligned} \langle \mathbf{r}|\, \mathbf{H}_{\text{KE}}^{(\text{GB})}\,|\Psi\rangle &\equiv \mathbf{H}_{\text{KE}}^{(\text{GB})}(\mathbf{r})\,\Psi(\mathbf{r}) \\ &\overset{\text{def}}{=} -\frac{\hbar^2}{4m_0}\left[\nabla^2\left(\frac{1}{m(\mathbf{r})}\Psi(\mathbf{r})\right) + \frac{1}{m(\mathbf{r})}\nabla^2\Psi(\mathbf{r})\right]. \end{aligned} \tag{3.21}$$

For either form of the KE operator, we solve Eqn. (3.19) for the wavefunction over the entire device in two steps:

1. We divide the device into regions and establish the form for $\Psi(\mathbf{r})$ within each as a linear combination of known basis functions and unknown coefficients in Section 4, and

2. We apply coupling-conditions at inter-region boundaries to arrive at constraints on the coefficients in Section 5 so that $\Psi(\mathbf{r})$ remains a global solution to the 3D-SBEM-TISE over the entire device.

Section 6 employs the results from these two sections to deduce simplified scattering conditions (diffraction) and a simple formula for transmitted phase current that naturally leads to an expression for the total current per unit-cell.

4. Region-wise wavefunction establishment . Regions comprising the device are conceptually classified as contacts, spacers or quantum dot layers (QDL) as discussed in Section 2.1. The following subsections establish the form of the wavefunction in each region.

4.1. Wavefunction in contacts. The isotropy of the contacts, simplifies Eqn. (3.19) (for both cases of the KE operator) to,

$$\left[-\frac{\hbar^2}{2m_0 m^{(\text{CON})}}\nabla^2 + V^{(\text{CON})}\right]\Psi(\mathbf{r}) = E\Psi(\mathbf{r}), \tag{4.1}$$

where $m^{(\text{CON})}$ is the (constant) relative effective mas. Allowed solutions are planewaves with wavevectors $\mathbf{k} \in \mathbb{R}^3$. During model development we take the wavefunction in the contacts to be a general superposition,

$$\Psi^{(\text{CON})}(\mathbf{r}; E) \stackrel{\text{def}}{=} \iint_{\mathbb{K}_{\parallel}^{(\text{CON})}(E)} \psi^{(\text{CON})}\left(z; E, \mathbf{k}_{\parallel}\right)\left\langle \mathbf{r}_{\parallel} \mid \mathbf{k}_{\parallel}\right\rangle d^2k_{\parallel}, \tag{4.2}$$

$$\begin{aligned}\psi^{(\text{CON})}\left(z; E, \mathbf{k}_{\parallel}\right) \stackrel{\text{def}}{=}\, & a^{(\text{CON})}\left(\mathbf{k}_{\parallel}\right) e^{ik_z^{(\text{CON})}\left(E,\mathbf{k}_{\parallel}\right)z} \\ & + b^{(\text{CON})}\left(\mathbf{k}_{\parallel}\right) e^{-ik_z^{(\text{CON})}\left(E,\mathbf{k}_{\parallel}\right)z}.\end{aligned} \tag{4.3}$$

The wavevector distribution includes only propagating phases and neglects evanescent phases because these are asymptotically negligible and do not contribute to probability current.

Eqns.(3.7) and (3.10) for an incident phase with wavevector $\mathbf{k}^{(\text{INC})} = \mathbf{k}_{\parallel}^{(\text{INC})} + k_z^{(\text{INC})}\hat{\mathbf{z}}$ are recovered from Eqn. (4.2) by imposing,

$$a^{(\text{INJ})}\left(\mathbf{k}_{\parallel}^{(\text{INC})}\right) = 2\pi\delta\left(\mathbf{k}_{\parallel} - \mathbf{k}_{\parallel}^{(\text{INC})}\right), \tag{4.4}$$

$$b^{(\text{TRA})}\left(\mathbf{k}_{\parallel}\right) \equiv 0. \tag{4.5}$$

Then, following the establishment of the wavefunction throughout the device and using $E = E^{(\text{INJ})}\left(\mathbf{k}^{(\text{INC})}\right)$ along with Eqn. (3.14) for the correct longitudinal wavevectors, we get

$$\rho\left(\mathbf{k}^{(\text{INC})}, \mathbf{k}_{\parallel} + k_z^{(\text{INJ})}\left(E, \mathbf{k}_{\parallel}\right)\hat{\mathbf{z}}\right) \quad \mapsto \quad (2\pi)^2\, b^{(\text{INJ})}\left(\mathbf{k}_{\parallel}\right), \tag{4.6}$$

$$\tau\left(\mathbf{k}^{(\text{INC})}, \mathbf{k}_{\parallel} + k_z^{(\text{TRA})}\left(E, \mathbf{k}_{\parallel}\right)\hat{\mathbf{z}}\right) \quad \mapsto \quad (2\pi)^2\, a^{(\text{TRA})}\left(\mathbf{k}_{\parallel}\right). \tag{4.7}$$

4.2. Wavefunction in spacers. Spacer and wetting-layers are similar to contacts except that the applied external voltage perturbs the PEF by $V_{\text{bias}}(z) = V_0 + V'z$, in a local $z-$coordinate system, where V_0 is the potential energy at the start of the region and V' is the potential energy gradient induced (assumed constant throughout the device). The longitudinal components of the wavefunction are now expressed in terms of Airy functions ([26, Chp. 7]) and the general wavefunction is a superposition of all allowed solutions,

$$\Psi^{(\text{SPC})}\left(\mathbf{r}_\parallel, z; E\right) = \iint_{\mathbb{K}} \psi^{(\text{SPC})}\left(z; E, \mathbf{k}_\parallel, V_0, V'\right) \left\langle \mathbf{r}_\parallel \mid \mathbf{k}_\parallel \right\rangle d^2 k_\parallel, \tag{4.8}$$

$$\begin{aligned}\psi^{(\text{SPC})}\left(z; E, \mathbf{k}_\parallel, V_0, V'\right) = {} & a^{(\text{SPC})}\left(\mathbf{k}_\parallel; E\right) \operatorname{Ai}\left(\sigma\left(z; E, \mathbf{k}_\parallel, V_0, V'\right)\right) \\ & + b^{(\text{SPC})}\left(\mathbf{k}_\parallel; E\right) \operatorname{Bi}\left(\sigma\left(z; E, \mathbf{k}_\parallel, V_0, V'\right)\right),\end{aligned} \tag{4.9}$$

$$\mathbb{K}_\parallel^{(\text{SPC})}(E) \stackrel{\text{def}}{=} \left\{\mathbf{k}_\parallel \in \mathbb{K} \mid E_z^{(\text{SPC})}\left(E, \mathbf{k}_\parallel\right) > 0\right\}, \tag{4.10}$$

$$E_z^{(\text{SPC})}\left(E, \mathbf{k}_\parallel\right) = E - \frac{\hbar^2 k_\parallel^2}{2 m_0 m^{(\text{SPC})}}, \tag{4.11}$$

$$\sigma\left(z; E, \mathbf{k}_\parallel, V_0, V'\right) \stackrel{\text{def}}{=} \sqrt[3]{\frac{2mV'}{\hbar^2}} \left(z - \frac{\left[E_z\left(E, \mathbf{k}_\parallel\right) - V_0\right]}{V'}\right), \tag{4.12}$$

where $a^{(\text{SPC})}\left(\mathbf{k}_\parallel; E\right)$ and $b^{(\text{SPC})}\left(\mathbf{k}_\parallel; E\right)$ are constants to be determined from boundary conditions. Unlike the case of contacts, lateral wavevectors are distributed over all of $\mathbb{K}$ - longitudinally evanescent states (for which $\sigma > 0$) represent tunneling contributions since the spacer regions are finite.

4.3. Wavefunction in QDL. The generality of quantum dot geometries (manifest in effective-mass and potential energy profiles), makes analytical solution possible only in very special cases. In this section we develop a two-step method to solve for a numerical approximation to the exact envelope function for general geometries in the QDL. We first make an exact transformation of the 3D-SBEM-TISE, which is a PDE of a scalar function in 3 spatial variables, to an infinite-dimensional (multi-component) vector ODE in spatial variable z alone. We then discretize along the z-axis and solve for the approximate wavefunction in each slice using a piecewise-constant approximation for the geometry.

4.3.1. Transformation of 3D-SBEM-TISE to 1D Vector ODE. In the QDL, $m(\mathbf{r})$ and $V(\mathbf{r})$ show 3D variation due to QD structure - lateral variation is periodic. In addition, $V(\mathbf{r})$ includes the 1D, linear contribution from the applied bias, i.e., $V(\mathbf{r}) = V_{\text{struct}}(\mathbf{r}) + V_{\text{bias}}(z)$. The restriction of the Hamiltonian to an arbitrary $z = z_0$ becomes,

$$\mathbf{H}\big|_{z=z_0} = \mathbf{H}_{\text{KE}}^{\parallel}\Big|_{z=z_0} + \mathbf{H}_{\text{KE}}^{\perp}\big|_{z=z_0} + \mathbf{V}_{\text{struct}}\big|_{z=z_0} + \mathbf{V}_{\text{bias}}\big|_{z=z_0}, \tag{4.13}$$

where the PEF and effective mass show periodic, lateral variation,

$$\begin{aligned} V_{\text{struct}}\left(\mathbf{r}_\parallel + \mathbf{R}_{\parallel lm}; z_0\right) &\equiv V_{\text{struct}}\left(\mathbf{r}_\parallel; z_0\right), \qquad (l, m) \in \mathbb{Z}^2 \\ m\left(\mathbf{r}_\parallel + \mathbf{R}_{\parallel lm}; z_0\right) &\equiv m\left(\mathbf{r}_\parallel; z_0\right),\end{aligned} \tag{4.14}$$

and $\mathbf{H}_{\mathrm{KE}}^{\|}$ contains all terms with no partial z-derivatives and $\mathbf{H}_{\mathrm{KE}}^{\perp}$ contains all terms with partial z-derivatives. Expressions for these operators for both cases of the KE operator are

$$\mathbf{H}_{\mathrm{KE}}^{(\mathrm{BD})\|}\left(\mathbf{r}_{\|};z_0\right)\,f\left(\mathbf{r}_{\|}\right)=-\frac{\hbar^2}{2m_0}\nabla_{\|}\bullet\left\{\frac{1}{m\left(\mathbf{r}_{\|};z_0\right)}\nabla_{\|}f\left(\mathbf{r}_{\|}\right)\right\} \tag{4.15}$$

$$\mathbf{H}_{\mathrm{KE}}^{(\mathrm{BD})\perp}\left(z;\mathbf{r}_{\|}\right)\,f\left(z\right)\Big|_{z=z_0}=-\frac{\hbar^2}{2m_0}\frac{\partial}{\partial z}\left\{\frac{1}{m\left(z;\mathbf{r}_{\|}\right)}\frac{\partial}{\partial z}f\left(z\right)\right\}\Bigg|_{z=z_0} \tag{4.16}$$

$$\begin{aligned}\mathbf{H}_{\mathrm{KE}}^{(\mathrm{GB})\|}\left(\mathbf{r}_{\|};z_0\right)f\left(\mathbf{r}_{\|}\right)\;=&\\ -\frac{\hbar^2}{4m_0}&\left[\nabla_{\|}^2\left\{\frac{1}{m\left(\mathbf{r}_{\|};z_0\right)}f\left(\mathbf{r}_{\|}\right)\right\}+\frac{1}{m\left(\mathbf{r}_{\|};z_0\right)}\nabla_{\|}^2f\left(\mathbf{r}_{\|}\right)\right],\end{aligned} \tag{4.17}$$

$$\begin{aligned}\mathbf{H}_{\mathrm{KE}}^{(\mathrm{GB})\perp}\left(z;\mathbf{r}_{\|}\right)f\left(z\right)\Big|_{z=z_0}\;=&\\ -\frac{\hbar^2}{4m_0}&\left[\frac{\partial^2}{\partial z^2}\left\{\frac{1}{m\left(z;\mathbf{r}_{\|}\right)}f\left(z\right)\right\}+\frac{1}{m\left(z;\mathbf{r}_{\|}\right)}\frac{\partial^2}{\partial z^2}f\left(z\right)\right]\Bigg|_{z=z_0}.\end{aligned} \tag{4.18}$$

To exploit the lateral symmetry, we define a new, local, laterally-periodic “Hamiltonian” operator $\mathbf{H}^{\|}\left(z_0\right)$ and invoke the Bloch theorem [1] to use $\mathbf{g}_{\|}\in\mho_{\|}$ and band-indices $n\in\mathbb{N}$ to index its eigenenergies and eigenfunctions,

$$\mathbf{H}^{\|}\Big|_{z=z_0}=\mathbf{H}_{\mathrm{KE}}^{\|}\Big|_{z=z_0}+\mathbf{V}_{\mathrm{struct}}\big|_{z=z_0}, \tag{4.19}$$

$$\mathbf{H}^{\|}\Big|_{z=z_0}\left|n\mathbf{g}_{\|}\left(z_0\right)\right\rangle=\varepsilon_{n\mathbf{g}_{\|}}\left(z_0\right)\left|n\mathbf{g}_{\|}\left(z_0\right)\right\rangle. \tag{4.20}$$

The representation and properties of these lateral eigenstates, discussed in Appendix B, are useful in subsequent derivations.

It can be proved that the lateral Hamiltonian $\mathbf{H}^{\|}\big|_{z=z_0}$ is hermitian when either form of the kinetic energy operator (Eqn. (3.20), Eqn. (3.21)) is used. In each case, we assume that the set $\mathbf{\Phi}\left(z\right)=\left\{\left|n\mathbf{g}_{\|}\left(z_0\right)\right\rangle\mid n\in\mathbb{N},\mathbf{g}_{\|}\in\mho_{\|}\right\}$ of lateral eigenfunctions forms a complete basis of orthogonal (without loss of generality, ortho*normal*) functions for representing well-behaved functions of $\mathbf{r}_{\|}$ - this should be the case for realistic effective-mass and potential energy distributions. Therefore, the restriction of the global 3D wavefunction $\Psi\left(\mathbf{r}\right)$ to $z=z_0$, which we denote as the ket $\left|\Psi\left(z_0\right)\right\rangle$, has a representation in this basis with (as yet unknown) complex-valued coordinates $c_{n\mathbf{g}_{\|}}\left(z_0\right)$,

$$\left|\Psi\left(z_0\right)\right\rangle\equiv\sum_{n\in\mathbb{N}}\iint_{\mho_{\|}}c_{n\mathbf{g}_{\|}}\left(z_0\right)\left|n\mathbf{g}_{\|}\left(z_0\right)\right\rangle\,d^2g_{\|}, \tag{4.21}$$

To determine these coefficients, we substitute (4.20) and Eqn. (4.21) into Eqn. (3.19) and rearrange to get,

$$\begin{aligned}\mathbf{H}_{KE}^{\perp}\left(z_0\right)\sum_{n\in\mathbb{N}}\iint_{\mho_{\|}}c_{n\mathbf{g}_{\|}}\left(z_0\right)\left|n\mathbf{g}_{\|}\left(z_0\right)\right\rangle d^2g_{\|}\;=&\\ \sum_{n\in\mathbb{N}}\iint_{\mho_{\|}}\left(E-V_{\mathrm{bias}}\left(z_0\right)-\varepsilon_{n\mathbf{g}_{\|}}\left(z_0\right)\right)c_{n\mathbf{g}_{\|}}&\left(z_0\right)\left|n\mathbf{g}_{\|}\left(z_0\right)\right\rangle d^2g_{\|}.\end{aligned} \tag{4.22}$$

After projecting both sides onto various $\left|n'\mathbf{g'}_{\|}\left(z_0\right)\right\rangle \in \mathbf{\Phi}\left(z\right)$, collecting the results, and generalizing z_0 to z, we get the following ODE for the vector of coefficients $\mathbf{c}\left(z\right)$,

$$\frac{d^2}{dz^2}\mathbf{c}\left(z\right)+\mathbf{P}\left(z\right)\frac{d}{dz}\mathbf{c}\left(z\right)+\left[\mathbf{Q}\left(z\right)+\mathbf{M}\left(z\right)\mathbf{K}_z^2\left(z\right)\right]\mathbf{c}\left(z\right)=\mathbf{0}. \tag{4.23}$$

The expressions for the matrix-elements of operators $\mathbf{P}\left(z\right)$, $\mathbf{Q}\left(z\right)$, $\mathbf{M}\left(z\right)$ and $\mathbf{K}_z^2\left(z\right)$ for both BenDaniel-Duke and G.Bastard forms of the KE operator are derived in Appendix C. The operators in this equation quantitatively relate the coupling between various modes to the evolution of their amplitudes in the wavefunction as we move along z. They are are therefore termed *local mode-coupling operators* for the QDL. Both $\mathbf{P}\left(z\right)$ and $\mathbf{Q}\left(z\right)$ explicitly capture the $z-$variation of the effective-mass profile. Operators $\mathbf{Q}\left(z\right)$ and $\mathbf{K}_z^2\left(z\right)$ implicitly capture the $z-$variation of the potential energy profile through the $z-$variation of the lateral wavefunctions and eigenenergies.

The matrix for $\mathbf{K}_z^2\left(z\right)$ is diagonal in the lateral eigenbasis. The matrices for $\mathbf{P}\left(z\right)$, $\mathbf{Q}\left(z\right)$ and $\mathbf{M}\left(z\right)$ assume block-diagonal form when the lateral eigenbasis at z is ordered according to a scheme where the eigenfunctions for all band-indices corresponding to each $\mathbf{g}_{\|}\in\mho_{\|}$ are clustered together (order is immaterial) for any linearized ordering of the elements in the Brillouin zone. We term such an order a natural order.

Definition 4.1. *A* natural order $\mathbf{\Phi}^{\leq}\left(z\right)$ *of the lateral eigenbasis* $\mathbf{\Phi}\left(z\right)$ *is the partially-ordered basis obtained by imposing a partial order* $\leq$ *over* $\mathbf{\Phi}\left(z\right)$ *such that,*

$$\forall\mathbf{g}_{\|},\mathbf{g'}_{\|}\in\mho_{\|},\ \forall n,n'\in\mathbb{N}:\ \left|n\mathbf{g}_{\|}\left(z\right)\right\rangle\leq\left|n'\mathbf{g'}_{\|}\right\rangle\quad \textit{if}\quad \mathbf{g}_{\|}<\mathbf{g'}_{\|},$$

for any total order $<$ *on the set* $\mho_{\|}$ *of Brillouin-zone vectors.*

In fact, this definition is equivalent to definition 2.3 due to the properties discussed in Appendix B. The block-diagonal structure of the local mode-coupling matrices in a natural order is proved in Appendix D.

For each $\mathbf{g}_{\|}\in\mho_{\|}$, the set $\mathbf{\Phi}_{\left[\mathbf{g}_{\|}\right]}\left(z\right)\stackrel{\text{def}}{=}\left\{\left|n\mathbf{g}_{\|}\left(z\right)\right\rangle\mid n\in\mathbb{N}\right\}\subset\mathbf{\Phi}\left(z\right)$ generates the BZV-subspace corresponding to $\mathbf{g}_{\|}$ as proved in proposition B.1 in Appendix B. Using the group-theoretic facts in Appendix A, Eqn. (4.23) can equivalently be expressed in a form that restricts all quantities to an arbitrary BZV-subspace,

$$\frac{d^2}{dz^2}\mathbf{c}_{\left[\mathbf{g}_{\|}\right]}\left(z\right)+\mathbf{P}_{\left[\mathbf{g}_{\|}\right]}\left(z\right)\frac{d}{dz}\mathbf{c}_{\left[\mathbf{g}_{\|}\right]}\left(z\right)+\mathbf{R}_{\left[\mathbf{g}_{\|}\right]}\mathbf{c}_{\left[\mathbf{g}_{\|}\right]}\left(z\right)=\mathbf{0}, \tag{4.24}$$

$$\mathbf{R}_{\left[\mathbf{g}_{\|}\right]}\left(z\right)\stackrel{\text{def}}{=}\mathbf{Q}_{\left[\mathbf{g}_{\|}\right]}\left(z\right)+\mathbf{M}_{\left[\mathbf{g}_{\|}\right]}\left(z\right)\mathbf{K}^2_{z\left[\mathbf{g}_{\|}\right]}\left(z\right). \tag{4.25}$$

Therefore, Eqn. (4.23) entirely block-diagonal in a natural ordering of the lateral eigenbasis. Concise expressions for the matrix elements in Eqn. (4.24) are derived in Appendix E.

Since there is no coupling between subspaces corresponding to differing $\mathbf{g}_{\|}$ at any value of z, computations on each $\mathbf{g}_{\|}$-block (BZV-subspace) can be performed independently of others. Hence it is unnecessary to actually impose any sort of total order on the elements of the Brillouin zone.

To eliminate the first derivative term from Eqn. (4.23), we introduce a new unknown vector $\boldsymbol{\chi}\left(z\right)$ which is related to $\mathbf{c}\left(z\right)$ by (an as yet unknown) linear transformation $\boldsymbol{\mathcal{C}}\left(z\right)$,

$$\mathbf{c}(z) \stackrel{\text{def}}{=} \boldsymbol{\mathcal{C}}(z)\,\boldsymbol{\chi}(z)\,, \tag{4.26}$$

$$\text{i.e., } c_{n\mathbf{g}_\parallel}(z) = \iint_{\mho_\parallel} \sum_{n'\in\mathbb{N}} \mathcal{C}_{n\mathbf{g}_\parallel,n'\mathbf{g}'_\parallel}(z)\ \chi_{n'\mathbf{g}'_\parallel}(z)\ d^2g_\parallel.$$

Then, substituting Eqn. (4.26) into Eqn. (4.23) and constraining $\boldsymbol{\mathcal{C}}(z)$ to respect,

$$\frac{d}{dz}\boldsymbol{\mathcal{C}}(z) = -\frac{1}{2}\mathbf{P}(z)\,\boldsymbol{\mathcal{C}}(z)\,. \tag{4.27}$$

we get,

$$\frac{d^2}{dz^2}\boldsymbol{\chi}(z) + \mathbf{W}(z)\,\boldsymbol{\chi}(z) = \mathbf{0}, \tag{4.28}$$

$$\mathbf{W}(z) = \boldsymbol{\mathcal{C}}^{-1}(z)\,\mathbf{G}(z)\,\boldsymbol{\mathcal{C}}(z)\,, \tag{4.29}$$

$$\mathbf{G}(z) = \mathbf{G}_0(z) + \mathbf{M}(z)\mathbf{K}_z^2(z)\,, \tag{4.30}$$

$$\mathbf{G}_0(z) = -\frac{1}{2}\frac{d}{dz}\mathbf{P}(z) - \frac{1}{4}\mathbf{P}^2(z) + \mathbf{Q}(z)\,. \tag{4.31}$$

Choosing initial condition $\mathbf{c}(0) = \boldsymbol{\chi}(0)$ for Eqn. (4.27) so that $\boldsymbol{\mathcal{C}}(0) = \mathbf{I}$ extends the block-diagonal nature of matrices for $\mathbf{P}(z)$, $\mathbf{Q}(z)$, and $\mathbf{M}(z)$ to the matrices for $\mathbf{W}(z)$, $\mathbf{G}(z)$, and $\mathbf{G}_0(z)$ in Eqns. (4.29)-(4.31) in a natural ordering of the lateral eigenbasis. Appendix E presents expressions for $\mathbf{G}_{0[\mathbf{g}_\parallel]}(z)$ for both forms of the KE operator. The fact that $\exists\boldsymbol{\mathcal{D}}(z) : \boldsymbol{\mathcal{C}}(z) \equiv \exp(\boldsymbol{\mathcal{D}}(z))$ is proved in [7]. For any such exponential, $\boldsymbol{\mathcal{C}}^{-1}(z) \equiv \exp(-\boldsymbol{\mathcal{D}}(z))$ is well-defined for any $\boldsymbol{\mathcal{D}}(z)$ [13].

4.3.2. Numerical solution procedure . We now divide the QDL into slices along the z-axis with slice thickness Δz being empirically selected to be so small that $\boldsymbol{\mathcal{C}}(z)$ and $\mathbf{G}(z)$ vary quasi-statically over this interval and are locally well-approximated by the $z-$invariant operators $\boldsymbol{\mathcal{C}}_j$ and $\mathbf{G}_j$ in the j^{th} slice $(j = 1, 2, \ldots)$, evaluated at the middle of the slice. Then, within each slice, Eqn. (4.28) takes the form,

$$\frac{d^2}{dz^2}\boldsymbol{\chi}_j(z) + \mathbf{W}_j\boldsymbol{\chi}_j(z) = \mathbf{0}, \qquad \mathbf{W}_j = \boldsymbol{\mathcal{C}}_j^{-1}\mathbf{G}_j\boldsymbol{\mathcal{C}}_j. \tag{4.32}$$

Because $\mathbf{W}_j$ is constant, the solution to this equation is of the form

$$\boldsymbol{\chi}_j(z) = \boldsymbol{\Theta}'_j\left[\exp(i\boldsymbol{\Xi}_j z)\,\mathbf{a}_j + \exp(-i\boldsymbol{\Xi}_j z)\,\mathbf{b}_j\right], \tag{4.33}$$

$$\mathbf{W}_j\boldsymbol{\Theta}'_j = \boldsymbol{\Theta}'_j\boldsymbol{\Xi}_j^2, \tag{4.34}$$

where we label $\mathbf{a}_j$ and $\mathbf{b}_j$ as the *advancing-mode coefficients* and *retreating-mode coefficients* resepectively, and the remaining terms come from the eigen-decomposition of $\mathbf{W}_j$ as per Eqn. (4.34) - $\boldsymbol{\Theta}'_j$ is analogous to the matrix of eigenvectors-as-columns in a finite-dimensional case, and $\boldsymbol{\Xi}_j^2$ is analogous to the diagonal matrix of eigenvalues. The values of the advancing and retreating mode-coefficients, when determined from boundary conditions, will completely establish the $\boldsymbol{\chi}_j(z)$.

Since $\mathbf{W}_j$ and $\mathbf{G}_j$ are related by the similarity transform in Eqn. (4.29), their eigenvalues are identical and their eigenvectors are related,

$$\mathbf{G}_j\mathbf{\Theta}_j = \mathbf{\Theta}_j\mathbf{\Xi}_j^2, \qquad \mathbf{\Theta}_j = \boldsymbol{\mathcal{C}}_j\mathbf{\Theta}'_j. \tag{4.35}$$

Therefore, using Eqn. (4.26) and Eqn. (4.35), Eqn. (4.33) yields,

$$\mathbf{c}_j(z) = \mathbf{\Theta}_j\left[\exp\left(i\mathbf{\Xi}_j z\right)\mathbf{a}_j + \exp\left(-i\mathbf{\Xi}_j z\right)\mathbf{b}_j\right]. \tag{4.36}$$

This equation expresses the longitudinal variations for various lateral modes within each slice, as linear combinations of advancing and retreating *effective* 1D planewaves (with complex-valued wavenumbers).

The approximate spatial behavior of the wavefunction within the j^{th} slice in a local $z-$coordinate system is therefore,

$$\Psi_j^{(\text{QDL})}\left(\mathbf{r}_\parallel, z_j\right) = \sum_{n\in\mathbb{N}}\iint_{\mho_\parallel} c_{j,n\mathbf{g}_\parallel}\left(z_j\right)\phi_{j,n\mathbf{g}_\parallel}\left(\mathbf{r}_\parallel\right)\, d^2g_\parallel,\ \ 0\le z_j\le l_j \tag{4.37}$$

where the $\phi_{j,n\mathbf{g}_\parallel}\left(\mathbf{r}_\parallel\right)$ denote spatial representation of the corresponding lateral eigenfunctions *in the equatorial lateral plane* of the j^{th} slice.

While the intermediate $\boldsymbol{\mathcal{C}}(z)$, introduced in Eqn. (4.26), does not appear explicitly in Eqn. (4.36), its presence is implicit in the structure of $\mathbf{\Theta}_j$. Because block-diagonality is preserved throughout, the above numerical procedure may actually be performed independently on restrictions to each BZV-subspace,

$$\mathbf{c}_{j\left[\mathbf{g}_\parallel\right]}(z) = \mathbf{\Theta}_{j\left[\mathbf{g}_\parallel\right]}\left[\exp\left(i\mathbf{\Xi}_{j\left[\mathbf{g}_\parallel\right]}z\right)\mathbf{a}_{j\left[\mathbf{g}_\parallel\right]} + \exp\left(-i\mathbf{\Xi}_{j\left[\mathbf{g}_\parallel\right]}z\right)\mathbf{b}_{j\left[\mathbf{g}_\parallel\right]}\right]. \tag{4.38}$$

This is the computationally simpler approach which has the twin advantages of being highly parallel and requiring much lesser memory than a naive implementation using Eqn. (4.36).

5. Inter-region wavefunction coupling . We now observe that in each three types of regions - contacts (Eqn. (4.2)), spacers (Eqn. (4.8)) and QDL slices (Eqn. (4.37)), the wavefunctions are linear combinations of known *modes* (indexed by a suitable variable ι with range $\mathbb{B}$). These modes are 3D basis functions that are separable into a *lateral* component $|\iota\rangle_\parallel$, and advancing/retreating *longitudinal* components $|\iota\rangle_\perp^{(\pm)}$,

$$|\Psi\rangle = \sum_{\iota\in\mathbb{B}}\left(a_\iota\,|\iota\rangle^{(+)} + b_\iota\,|\iota\rangle^{(-)}\right) \tag{5.1}$$

$$|\iota\rangle^{(\pm)} \stackrel{\text{def}}{=} |\iota\rangle_\parallel\,|\iota\rangle_\perp^{(\pm)} \tag{5.2}$$

where the a_ι and the b_ι denote the (as yet unknown) advancing- and retreating- mode coefficients respectively within slices. Table 5.1 clarifies the spatial behavior of these modes in each region. The set of lateral components forms a complete, orthonormal basis for $\mathcal{F}$ in each case. Coefficients in adjacent regions are related by the continuity of the wavefunction and its associated probability current across the interface [5, 4] - a requirement imposed by the forms of the Hamiltonian for both KE operators.

	Contact	Spacer	QDL
ι	$\mathbf{k}_\parallel$	$\mathbf{k}_\parallel$	$\left(n, \mathbf{g}_\parallel\right)$
$\mathbb{B}$	$\mathbb{K}$	$\mathbb{K}$	$\mathbb{N} \times \mho_\parallel$
$\left\langle \mathbf{r}_\parallel \mid \iota \right\rangle_\parallel$	$\frac{1}{2\pi} e^{i\mathbf{k}_\parallel \bullet \mathbf{r}_\parallel}$	$\frac{1}{2\pi} e^{i\mathbf{k}_\parallel \bullet \mathbf{r}_\parallel}$	$\phi_{n\mathbf{g}_\parallel}\left(\mathbf{r}_\parallel; z\right)$
$\left\langle z \mid \iota \right\rangle_\perp^{(+)}$	$e^{ik_z\left(E,\mathbf{k}_\parallel\right)z}$	$\mathrm{Ai}\left(z; \mathbf{k}_\parallel, E, V_0, V'\right)$	$\left\{\mathbf{\Theta} \exp\left(i\mathbf{\Xi} z\right)\right\}_{n\mathbf{g}_\parallel}$
$\left\langle z \mid \iota \right\rangle_\perp^{(-)}$	$e^{-ik_z\left(E,\mathbf{k}_\parallel\right)z}$	$\mathrm{Bi}\left(z; \mathbf{k}_\parallel, E, V_0, V'\right)$	$\left\{\mathbf{\Theta} \exp\left(-i\mathbf{\Xi} z\right)\right\}_{n\mathbf{g}_\parallel}$

TABLE 5.1

Spatial representations for basis modes for the three types of regions

Let J denote the total number of regions between the contacts with the injecting contact at index 0 and the transmitting contact at index $J+1$. We use $j \in [0, 1, \ldots, J+1]$ as the region-index, especially as subscript on various quantities. Let l_j denote the length of region j and $z_j \in [0, l_j]$ denote the local z-coordinate within it. The boundary conditions to be enforced at its interface with region $j+1$ are,

$$\Psi_j\left(\mathbf{r}_\parallel, z_j\right)\Big|_{z_j=l_j} = \Psi_{j+1}\left(\mathbf{r}_\parallel, z_{j+1}\right)\Big|_{z_{j+1}=0}, \tag{5.3}$$

$$\frac{1}{m_j\left(\mathbf{r}_{||}; z_j\right)} \frac{\partial}{\partial z} \Psi_j\left(\mathbf{r}_\parallel, z_j\right)\Bigg|_{z_j=l_j} = \frac{1}{m_{j+1}\left(\mathbf{r}_{||}; z_{j+1}\right)} \frac{\partial}{\partial z} \Psi_{j+1}\left(\mathbf{r}_\parallel, z_{j+1}\right)\Bigg|_{z_{j+1}=0}. \tag{5.4}$$

At this interface, using Eqn. (5.1) in Eqn. (5.3) and Eqn. (5.4) we may express each $a_{j+1,\iota}$ and $b_{j+1,\iota}$ in terms of all the $a_{j,\iota'}$ and $b_{j,\iota'}$ by projecting both sides onto the $\left|\iota\right\rangle_{\parallel j+1}$,

$$\begin{bmatrix} \left\langle 0 \mid \iota \right\rangle_{\perp j+1}^{(+)} & \left\langle 0 \mid \iota \right\rangle_{\perp j+1}^{(-)} \\ \left\langle 0 \right| \frac{d}{dz} \left|\iota\right\rangle_{\perp j+1}^{(+)} & \left\langle 0 \right| \frac{d}{dz} \left|\iota\right\rangle_{\perp j+1}^{(-)} \end{bmatrix} \begin{bmatrix} a_{j+1,\iota} \\ b_{j+1,\iota} \end{bmatrix} = \sum_{\iota' \in \mathbb{B}_j} \begin{bmatrix} x_{1\ \iota,\iota'}^{(j+1,j)} & 0 \\ 0 & x_{2\ \iota,\iota'}^{(j+1,j)} \end{bmatrix} \begin{bmatrix} \left\langle l_j \mid \iota' \right\rangle_{\perp j}^{(+)} & \left\langle l_j \mid \iota' \right\rangle_{\perp j}^{(-)} \\ \left\langle l_j \right| \frac{d}{dz} \left|\iota'\right\rangle_{\perp j}^{(+)} & \left\langle l_j \right| \frac{d}{dz} \left|\iota'\right\rangle_{\perp j}^{(-)} \end{bmatrix} \begin{bmatrix} a_{j,\iota'} \\ b_{j,\iota'} \end{bmatrix}, \tag{5.5}$$

where,

$$x_{1\ \iota,\iota'}^{(j+1,j)} \stackrel{\text{def}}{=} \left\langle (\iota)_{j+1} \mid (\iota')_j \right\rangle = \iint_{\mathbb{R}^2} \phi_{j+1,\,\iota}^*\left(\mathbf{r}_\parallel\right) \phi_{j,\,\iota'}\left(\mathbf{r}_\parallel\right)\, d^2 r_\parallel, \tag{5.6}$$

$$x_{2\ \iota,\iota'}^{(j+1,j)} \stackrel{\text{def}}{=} \left\langle (\iota)_{j+1} \right| \mathbf{M}_{j+1} \mathbf{M}_j^{-1} \left| (\iota')_j \right\rangle = \iint_{\mathbb{R}^2} \phi_{j+1,\,\iota}^*\left(\mathbf{r}_\parallel\right) \frac{m_{j+1}\left(\mathbf{r}_\parallel\right)}{m_j\left(\mathbf{r}_\parallel\right)} \phi_{j,\,\iota'}\left(\mathbf{r}_\parallel\right) d^2 r_\parallel. \tag{5.7}$$

The above equations represent forward-scattering of the (amplitudes of) components in region j into components in region $j+1$, and may be recast as,

$$\begin{bmatrix} a_{j+1,\iota} \\ b_{j+1,\iota} \end{bmatrix} = \sum_{\iota' \in \mathbb{B}_j} \mathbf{T}_{(j+1,\,j)\,\iota,\iota'} \begin{bmatrix} a_{j,\iota'} \\ b_{j,\iota'} \end{bmatrix} \tag{5.8}$$

where the $\mathbf{T}_{(j+1,\,j)\,\iota,\iota'}$ are the *inter-mode transfer matrices*. Defining $\mathbf{d}_j$ to be the vector of all coefficients in region j, the above equation may be written as,

$$
\begin{aligned}
\mathbf{d}_{j+1} &= \mathbf{T}_{(j+1,\,j)}\mathbf{d}_j, \\
\mathbf{T}_{(j+1,\,j)} &\stackrel{\text{def}}{=} \sum_{\substack{\iota\,\in\,\mathbb{B}_{j+1}\\ \iota'\,\in\,\mathbb{B}_j}} |\iota\rangle_{\parallel}\,\langle\iota'|_{\parallel} \otimes \mathbf{T}_{(j+1,\,j)\,\iota,\iota'},
\end{aligned}
\tag{5.9}
$$

where $\mathbf{T}_{(j+1,\,j)}$ is the *transfer operator* or *T-operator* for the interface. Back-scattering from modes $|\iota'\rangle_{j+1}$ to modes $|\iota\rangle_j$ is described by the inverse of the above T-matrix,

$$
\begin{aligned}
\mathbf{d}_j &= \mathbf{T}_{(j,\,j+1)}\mathbf{d}_{j+1}, \\
\mathbf{T}_{(j,\,j+1)} &= \mathbf{T}^{-1}_{(j+1,\,j)}.
\end{aligned}
$$

The T-operator is, in general, a linear transformation from the space $\mathcal{F}\otimes\mathbb{C}^2$ to itself.

Definition 5.1. *In this section, unless mentioned otherwise, the terms* space *and* subspace *refer to* $\mathcal{F}\otimes\mathbb{C}^2$ *and its subspaces, and not to* $\mathcal{F}$ *and its subspaces.* The definitions of natural order and BZV subspaces can intuitively be extended to $\mathcal{F}\otimes\mathbb{C}^2$. Let $\mathbf{\Phi} \stackrel{\text{def}}{=} \left\{|\iota\rangle_{\parallel} \mid \iota\in\mathbb{B}\right\}$ denote a basis for $\mathcal{F}$ in some region. Let $\mathbf{\Phi}_{[\mathbf{g}_\parallel]}$ denote a basis for $\mathcal{F}_{[\mathbf{g}_\parallel]}$ in that region and let $\mathbb{B}_{[\mathbf{g}_\parallel]}$ denote the set of indices corresponding to the elements in $\mathbf{\Phi}_{[\mathbf{g}_\parallel]}$. For example, in spacers and contacts, $\mathbb{B}_{[\mathbf{g}_\parallel]} = \mathbb{G}_{[\mathbf{g}_\parallel]}$ and $\mathbf{\Phi}_{[\mathbf{g}_\parallel]} = \mathcal{G}_{[\mathbf{g}_\parallel]}$ whereas in a QDL slice, $\mathbb{B}_{[\mathbf{g}_\parallel]} = \left\{\left(n,\mathbf{g}_\parallel\right) \mid n\in\mathbb{N}\right\}$ and $\mathbf{\Phi}_{[\mathbf{g}_\parallel]} = \left\{\left|n\mathbf{g}_\parallel\right\rangle \mid n\in\mathbb{N}\right\}$. Let $\mathbb{E} \stackrel{\text{def}}{=} \left\{\mathbf{e}_1 \stackrel{\text{def}}{=} \begin{bmatrix}1\\0\end{bmatrix}, \mathbf{e_2} \stackrel{\text{def}}{=} \begin{bmatrix}0\\1\end{bmatrix}\right\}$ denote a basis for $\mathbb{C}^2$.

Definition 5.2. *The spaces* $\mathcal{F}_{[\mathbf{g}_\parallel]}\otimes\mathbb{C}^2$ *are termed Brillouin-zone-vector (or BZV-) subspaces of* $\mathcal{F}\otimes\mathbb{C}^2$.

Definition 5.3. *A* natural order *of the basis-set* $\mathbf{\Phi}\otimes\mathbb{E} \stackrel{def}{=} \{|\iota\rangle\otimes\mathbf{e} \,|\, \iota\in\mathbb{B}\,,\,\mathbf{e}\in\mathbb{E}\}$ *for* $\mathcal{F}\otimes\mathbb{C}^2$ *is the partially-ordered basis-set obtained by imposing a partial order* $\leqq$ *on* $\mathbf{\Phi}\otimes\mathbb{E}$ *which is the extension of a natural order* $\leq$ *defined on* $\mathbf{\Phi}$*,*

$$
\forall\iota,\iota'\in\mathbb{B},\ \ \forall\mathbf{e},\mathbf{e}'\in\mathbb{E}\ :\qquad |\iota\rangle\otimes\mathbf{e}\ \leqq\ |\iota'\rangle\otimes\mathbf{e}'\quad \textit{if}\quad \iota\leq\iota'.
$$

As we prove in the following subsections, the T-operator assumes convenient, block-partitioned representations in certain orderings of the basis elements of the domain and range. We now define these basis-set-ordering relations.

Definition 5.4. *For the BZV subspace* $\mathcal{F}_{[\mathbf{g}_\parallel]}\otimes\mathbb{C}^2$ *corresponding to any* $\mathbf{g}_\parallel\in\mho_\parallel$*, a* mode-major order *of its basis-set* $\mathbf{\Phi}_{[\mathbf{g}_\parallel]}\otimes\mathbb{E} \stackrel{def}{=} \left\{|\iota\rangle\otimes\mathbf{e}\,|\,\iota\in\mathbb{B}_{[\mathbf{g}_\parallel]}\,,\,\mathbf{e}\in\mathbb{E}\right\}$ *is the partially-ordered basis obtained by imposing a partial order* $\leq_m$ *on* $\mathbf{\Phi}_{[\mathbf{g}_\parallel]}\otimes\mathbb{E}$*, defined such that,*

$$
\forall\iota,\iota'\in\mathbb{B}_{[\mathbf{g}_\parallel]}\,\forall\mathbf{e},\mathbf{e}'\in\mathbb{E}\ :\qquad |\iota\rangle\otimes\mathbf{e}\leq_m|\iota'\rangle\otimes\mathbf{e}'\quad \textit{if}\quad \iota<_m\iota',
$$

for any total order $<_m$ *on* $\mathbb{B}_{[\mathbf{g}_\parallel]}$.

Definition 5.5. *For the BZV subspace* $\mathcal{F}_{[\mathbf{g}_\parallel]}\otimes\mathbb{C}^2$ *corresponding to any* $\mathbf{g}_\parallel\in\mho_\parallel$*, a* component-major order *of the basis-set* $\mathbf{\Phi}_{[\mathbf{g}_\parallel]}\otimes\mathbb{E} \stackrel{def}{=} \left\{|\iota\rangle\otimes\mathbf{e}\,|\,\iota\in\mathbb{B}_{[\mathbf{g}_\parallel]}\,,\,\mathbf{e}\in\mathbb{E}\right\}$ *is* *the partially-ordered basis obtained by imposing a partial order* $\leq_c$ *on* $\mathbf{\Phi}_{[\mathbf{g}_\parallel]}\otimes\mathbb{E}$*, defined such that,*

$$\forall\iota,\iota'\in\mathbb{B}_{[\mathbf{g}_\parallel]},\ \forall\mathbf{e},\mathbf{e}'\in\mathbb{E}\ :\qquad |\iota\rangle\otimes\mathbf{e}\leq_c|\iota'\rangle\otimes\mathbf{e}'\quad \textit{if}\quad \mathbf{e}<_c\ \mathbf{e}',$$

for any total order $<_c$ *on* $\mathbb{E}$*. For simplicity, we take* $\mathbf{e}_1\ <_c\ \mathbf{e}_2$*.* Definition 5.4 clusters the basis elements $\{|\iota\rangle\otimes\mathbf{e}_1,|\iota\rangle\otimes\mathbf{e}_2\}$, for each index ι. The T-matrix resulting from this order follows in an obvious manner from Eqn. (5.8), in terms smaller of 2×2 inter-mode T-matrices for each combination of source and destination modes. On the other hand, definition 5.5 clusters the basis elements $\{|\iota\rangle\otimes\mathbf{e},|\iota'\rangle\otimes\mathbf{e},\ldots\}$, with $\iota,\iota',\ldots\in\mathbb{B}_{[\mathbf{g}_\parallel]}$, for each $\mathbf{e}\in\mathbb{E}$, and makes the T-matrix a 2×2 block-partitioned matrix where each block relates the full set of advancing or retreating source components to the full set of advancing or retreating destination components,

$$\begin{bmatrix}\mathbf{a}_{j+1}\\ \mathbf{b}_{j+1}\end{bmatrix}=\mathbf{T}_{(j+1,\,j)}\begin{bmatrix}\mathbf{a}_{j}\\ \mathbf{b}_{j}\end{bmatrix},\tag{5.10}$$

$$\mathbf{T}_{(j+1,\,j)}\equiv\begin{bmatrix}\mathbf{T}_{(j+1,\,j)\,a\leftarrow a} & \mathbf{T}_{(j+1,\,j)\,b\leftarrow a}\\ \mathbf{T}_{(j+1,\,j)\,a\leftarrow b} & \mathbf{T}_{(j+1,\,j)\,b\leftarrow b}\end{bmatrix}$$

Subsections 5.1-5.5 prove that the lateral translational symmetry in the device leads to very specific patterns of inter-region mode-coupling at all types of interfaces, and derive concise expressions for the respective local transfer matrices. Section 5.6 consolidates these results to arrive at the properties of the global transfer matrix that couples the wavefunction coefficients at both contacts.

5.1. Inter-slice coupling in QDL . Applying the general T-matrix procedure at an inter-slice boundary within a QDL, we arrive at the following results. Details of the derivation are provided in Appendix F.1.

THEOREM 5.6. *At the interface between two adjacent QDL slices, with region indices* j *and* $j+1$*, inter-region coupling occurs only between modes whose indices share the same Brillouin-zone-vector, i.e., for each* $\mathbf{g}_\parallel\in\mho_\parallel$*, modes* $\left|n\mathbf{g}_\parallel\right\rangle_j$ *couple only to modes* $\left|n'\mathbf{g}_\parallel\right\rangle_{j+1}$*, for all* $n,n'\in\mathbb{N}$*, and vice-versa. There is no coupling between modes* $\left|n\mathbf{g}_\parallel\right\rangle_j$ *and* $\left|n'\mathbf{g}'_\parallel\right\rangle_{j+1}$ *when* $\mathbf{g}_\parallel\neq\mathbf{g}'_\parallel$ *(*$\mathbf{g}'_\parallel\in\mho_\parallel$*) for all* $n,n'\in\mathbb{N}$*.*

The expression for the restriction of the local T-matrix to an arbitrary BZV-subspace ($\mathbf{g}_\parallel\in\mho_\parallel$) is, with component-major basis-order,

$$\begin{bmatrix}\mathbf{a}^{(\mathrm{QDL})}_{j+1[\mathbf{g}_\parallel]}\\ \mathbf{b}^{(\mathrm{QDL})}_{j+1[\mathbf{g}_\parallel]}\end{bmatrix}\stackrel{\mathrm{def}}{=}\mathbf{T}^{(\mathrm{QDL|QDL})}_{(j+1,j)[\mathbf{g}_\parallel]}\begin{bmatrix}\mathbf{a}^{(\mathrm{QDL})}_{j[\mathbf{g}_\parallel]}\\ \mathbf{b}^{(\mathrm{QDL})}_{j[\mathbf{g}_\parallel]}\end{bmatrix},\tag{5.11}$$

$$\begin{aligned}\mathbf{T}^{(\mathrm{QDL|QDL})}_{(j+1,\,j)[\mathbf{g}_\parallel]}&=\frac{1}{2}\begin{bmatrix}\mathbf{I}&\mathbf{I}\\ \mathbf{I}&-\mathbf{I}\end{bmatrix}\begin{bmatrix}\mathbf{I}&\mathbf{0}\\ \mathbf{0}&\mathbf{\Xi}^{-1}_{j+1[\mathbf{g}_\parallel]}\end{bmatrix}\begin{bmatrix}\mathbf{\Theta}^{-1}_{j+1[\mathbf{g}_\parallel]}&\mathbf{0}\\ \mathbf{0}&\mathbf{\Theta}^{-1}_{j+1[\mathbf{g}_\parallel]}\end{bmatrix}\\ &\times\begin{bmatrix}\mathbf{X}^{(\mathrm{QDL|QDL})}_{1(j+1,\,j)[\mathbf{g}_\parallel]}&\mathbf{0}\\ \mathbf{0}&\mathbf{X}^{(\mathrm{QDL|QDL})}_{2(j+1,\,j)[\mathbf{g}_\parallel]}\end{bmatrix}\begin{bmatrix}\mathbf{\Theta}_{j[\mathbf{g}_\parallel]}&\mathbf{0}\\ \mathbf{0}&\mathbf{\Theta}_{j[\mathbf{g}_\parallel]}\end{bmatrix}\\ &\times\begin{bmatrix}\mathbf{I}&\mathbf{0}\\ \mathbf{0}&\mathbf{\Xi}_{j[\mathbf{g}_\parallel]}\end{bmatrix}\begin{bmatrix}\mathbf{I}&\mathbf{I}\\ \mathbf{I}&-\mathbf{I}\end{bmatrix}\begin{bmatrix}\exp\left(i\mathbf{\Xi}_{j[\mathbf{g}_\parallel]}l_j\right)&\mathbf{0}\\ \mathbf{0}&\exp\left(-i\mathbf{\Xi}_{j[\mathbf{g}_\parallel]}l_j\right)\end{bmatrix},\end{aligned}\tag{5.12}$$

where the matrix elements for the exchange operators are,

$$X^{(\mathrm{QDL|QDL})}_{1(j+1,\,j)\left[\mathbf{g}_{\|}\right]\,n_1 n_2} = \hat{\mathbf{u}}^{*}_{j+1,n_1\mathbf{g}_{\|}} \bullet \hat{\mathbf{u}}_{j,n_2\mathbf{g}_{\|}}, \tag{5.13}$$

$$X^{(\mathrm{QDL|QDL})}_{2(j+1,\,j)\left[\mathbf{g}_{\|}\right]\,n_1 n_2} = \hat{\mathbf{u}}^{*}_{j+1,n_1\mathbf{g}_{\|}} \bullet \left[\hat{\mathbf{m}}^{(\mathrm{QDL|QDL})}_{(j+1,\,j)} \odot \hat{\mathbf{u}}_{j,n_2\mathbf{g}_{\|}}\right], \tag{5.14}$$

$$m^{(\mathrm{QDL|QDL})}_{(j+1,\,j)}\left(\mathbf{r}_{\|}\right) \stackrel{\mathrm{def}}{=} \frac{m^{(\mathrm{QDL})}_{j+1}\left(\mathbf{r}_{\|}\right)}{m^{(\mathrm{QDL})}_{j}\left(\mathbf{r}_{\|}\right)} \equiv \sum_{(l,m)\in\mathbb{Z}^2} \hat{m}^{(\mathrm{QDL|QDL})}_{(j+1,\,j)lm} e^{i\mathbf{G}_{\|lm}\bullet\mathbf{r}_{\|}}. \tag{5.15}$$

From the structure of the T-matrix above, we draw the following conclusion.

Corollary 5.7. *The BZV-subspaces* $\mathcal{F}_{\left[\mathbf{g}_{\|}\right]}\otimes\mathbb{C}^2$, $\mathbf{g}_{\|}\in\mho_{\|}$, *are irreducible invariant subspaces for* $\mathbf{T}^{(QDL|QDL)}_{(j+1,\,j)}$. *The local T-operator is the direct-sum of its restrictions to all BZV subspaces and its matrix-representation is block-diagonal in a natural order of the eigenbases in both slices resulting from the imposition of the same total order* $<$ *on* $\mho_{\|}$,

$$\mathbf{T}^{(QDL|QDL)}_{(j+1,\,j)} \equiv \bigoplus_{\mathbf{g}_{\|}\in\mho_{\|}} \mathbf{T}^{(QDL|QDL)}_{(j+1,\,j)\left[\mathbf{g}_{\|}\right]}. \tag{5.16}$$

5.2. Spacer-QDL coupling . Applying the general T-matrix procedure at the interface between a spacer at index j and a QDL at index $j' = j \pm 1$, we arrive at the following results. Details of the derivation and new notation are provided in Appendix F.2.

Theorem 5.8. *At the interface between a spacer and a QDL, for each* $\mathbf{g}_{\|}\in\mho_{\|}$, *coupling occurs only between spacer-region modes with lateral behavior* $\left|\mathbf{g}_{\|lm}\right\rangle = \left|\mathbf{g}_{\|}+\mathbf{G}_{\|lm}\right\rangle$, $(l,m)\in\mathbb{Z}^2$, *and QDL modes with lateral behavior* $\left|n\mathbf{g}_{\|}\right\rangle$, $n\in\mathbb{N}$. *There is no coupling between spacer modes with lateral behavior* $\left|\mathbf{g}_{\|lm}\right\rangle$ *and QDL modes with lateral behavior* $\left|n\mathbf{g}'_{\|}\right\rangle$, *for all* $n\in\mathbb{N}$, $(l,m)\in\mathbb{Z}^2$, *when* $\mathbf{g}_{\|}\neq\mathbf{g}'_{\|}$.

Corollary 5.9. *The BZV-subspaces* $\mathcal{F}_{\left[\mathbf{g}_{\|}\right]}\otimes\mathbb{C}^2$, $\mathbf{g}_{\|}\in\mho_{\|}$, *are irreducible invariant subspaces for* $\mathbf{T}^{(QDL|SPC)}_{(j+1,\,j)}$ *and* $\mathbf{T}^{(SPC|QDL)}_{(j+1,\,j)}$. *The local transfer operators are the direct sum of their restrictions to all BZV-subspaces and are block-diagonal in natural ordering of eigenbases in both regions resulting from the imposition of the same total order* $<$ *on* $\mho_{\|}$.

$$\mathbf{T}^{(QDL|SPC)}_{(j+1,\,j)} \equiv \bigoplus_{\mathbf{g}_{\|}\in\mho_{\|}} \mathbf{T}^{(QDL|SPC)}_{(j+1,\,j)\left[\mathbf{g}_{\|}\right]}, \tag{5.17}$$

$$\mathbf{T}^{(SPC|QDL)}_{(j+1,\,j)} \equiv \bigoplus_{\mathbf{g}_{\|}\in\mho_{\|}} \mathbf{T}^{(SPC|QDL)}_{(j+1,\,j)\left[\mathbf{g}_{\|}\right]}. \tag{5.18}$$

5.2.1. Spacer-to-QDL coupling. Using theorem 5.8 and corollary 5.9, it suffices to provide the expression for the restriction of the T-matrix to an arbitrary BZV subspace. For some $\mathbf{g}_{\|}\in\mho_{\|}$, with component-major basis-order,

$$\begin{bmatrix} \mathbf{a}^{(\mathrm{QDL})}_{j+1\left[\mathbf{g}_{\|}\right]} \\ \mathbf{b}^{(\mathrm{QDL})}_{j+1\left[\mathbf{g}_{\|}\right]} \end{bmatrix} \stackrel{\mathrm{def}}{=} \mathbf{T}^{(\mathrm{QDL|SPC})}_{(j+1,\,j)\left[\mathbf{g}_{\|}\right]} \begin{bmatrix} \mathbf{a}^{(\mathrm{SPC})}_{j\left[\mathbf{g}_{\|}\right]} \\ \mathbf{b}^{(\mathrm{SPC})}_{j\left[\mathbf{g}_{\|}\right]} \end{bmatrix}, \tag{5.19}$$

$$\mathbf{T}^{(\mathrm{QDL|SPC})}_{(j+1,\,j)\left[\mathbf{g}_{\parallel}\right]} = \frac{1}{2}\begin{bmatrix} \mathbf{I} & \mathbf{I} \\ \mathbf{I} & -\mathbf{I} \end{bmatrix} \begin{bmatrix} \mathbf{I} & \mathbf{0} \\ \mathbf{0} & -i\boldsymbol{\Xi}^{-1}_{j+1\left[\mathbf{g}_{\parallel}\right]} \end{bmatrix}$$
$$\times \begin{bmatrix} \boldsymbol{\Theta}^{-1}_{j+1\left[\mathbf{g}_{\parallel}\right]} & \mathbf{0} \\ \mathbf{0} & \boldsymbol{\Theta}^{-1}_{j+1\left[\mathbf{g}_{\parallel}\right]} \end{bmatrix} \begin{bmatrix} \mathbf{X}^{(\mathrm{QDL|SPC})}_{1(j+1,\,j)\left[\mathbf{g}_{\parallel}\right]} & \mathbf{0} \\ \mathbf{0} & \mathbf{X}^{(\mathrm{QDL|SPC})}_{2(j+1,\,j)\left[\mathbf{g}_{\parallel}\right]} \end{bmatrix}$$
$$\times \begin{bmatrix} \mathbf{A}_{j\left[\mathbf{g}_{\parallel}\right]}\left(l_j; E, V_{0j}, V'\right) & \mathbf{B}_{j\left[\mathbf{g}_{\parallel}\right]}\left(l_j; E, V_{0j}, V'\right) \\ \mathbf{A}'_{j\left[\mathbf{g}_{\parallel}\right]}\left(l_j; E, V_{0j}, V'\right) & \mathbf{B}'_{j\left[\mathbf{g}_{\parallel}\right]}\left(l_j; E, V_{0j}, V'\right) \end{bmatrix}, \tag{5.20}$$

where the matrix elements for the exchange operators $\mathbf{X}^{(\mathrm{QDL|SPC})}_{1(j+1,j)}$ and $\mathbf{X}^{(\mathrm{QDL|SPC})}_{2(j+1,j)}$ are,

$$X^{(\mathrm{QDL|SPC})}_{1(j+1,\,j)\left[\mathbf{g}_{\parallel}\right]n,lm} = \hat{u}^{*}_{j+1,n\mathbf{g}_{\parallel},lm}, \tag{5.21}$$

$$X^{(\mathrm{QDL|SPC})}_{2(j+1,\,j)\left[\mathbf{g}_{\parallel}\right]n,lm} = \left(\hat{\mathbf{m}}^{(\mathrm{QDL|SPC})}_{(j+1,\,j)} \odot \hat{\mathbf{u}}^{*}_{j+1,n\mathbf{g}_{\parallel}}\right)_{lm}, \tag{5.22}$$

$$m^{(\mathrm{QDL|SPC})}_{(j+1,\,j)}\left(\mathbf{r}_{\parallel}\right) = \frac{m^{(\mathrm{QDL})}_{j+1}\left(\mathbf{r}_{\parallel}\right)}{m^{(\mathrm{SPC})}_{j}} \tag{5.23}$$

and $\hat{\mathbf{m}}^{(\mathrm{QDL|SPC})}_{(j+1,\,j)}$ denotes the vector of Fourier-series coefficients for the periodic ratio-of-effective-masses function $m^{(\mathrm{QDL|SPC})}_{(j+1,\,j)}\left(\mathbf{r}_{\parallel}\right)$. The Airy function operators in Eqn. (5.20) have diagonal matrix representation with elements,

$$A_{j\left[\mathbf{g}_{\parallel}\right]lm,lm}\left(l_j; \mathbf{g}_{\parallel}, E, V_{0j}, V'\right) = \mathrm{Ai}\left(\sigma\left(l_j; \mathbf{g}_{\parallel lm}, E, V_{0j}, V'\right)\right), \tag{5.24}$$

with similar expressions for $\mathbf{A}'_{j\left[\mathbf{g}_{\parallel}\right]}\left(l_j; E, V_{0j}, V'\right)$, $\mathbf{B}_{j\left[\mathbf{g}_{\parallel}\right]}\left(l_j; E, V_{0j}, V'\right)$ and $\mathbf{B}'_{j\left[\mathbf{g}_{\parallel}\right]}\left(l_j; E, V_{0j}, V'\right)$. Here, V_{0j} is the potential energy at $z_j = 0$.

5.2.2. QDL-to-spacer coupling . The local T-matrix, restricted to an arbitrary BZV-subspace $\left(\mathbf{g}_{\parallel} \in \mho_{\parallel}\right)$ with component-major basis-order, is

$$\begin{bmatrix} \mathbf{a}^{(\mathrm{SPC})}_{j+1\left[\mathbf{g}_{\parallel}\right]} \\ \mathbf{b}^{(\mathrm{SPC})}_{j+1\left[\mathbf{g}_{\parallel}\right]} \end{bmatrix} \stackrel{\mathrm{def}}{=} \mathbf{T}^{(\mathrm{SPC|QDL})}_{(j+1,\,j)\left[\mathbf{g}_{\parallel}\right]} \begin{bmatrix} \mathbf{a}^{(\mathrm{QDL})}_{j\left[\mathbf{g}_{\parallel}\right]} \\ \mathbf{b}^{(\mathrm{QDL})}_{j\left[\mathbf{g}_{\parallel}\right]} \end{bmatrix}, \tag{5.25}$$

$$\mathbf{T}^{(\mathrm{SPC|QDL})}_{(j+1,\,j)\left[\mathbf{g}_{\parallel}\right]} = \begin{bmatrix} \mathbf{A}_{j+1\left[\mathbf{g}_{\parallel}\right]}\left(0; \mathbf{g}_{\parallel}, E, V_{0(j+1)}, V'\right) & \mathbf{B}_{j+1\left[\mathbf{g}_{\parallel}\right]}\left(0; \mathbf{g}_{\parallel}, E, V_{0(j+1)}, V'\right) \\ \mathbf{A}'_{j+1\left[\mathbf{g}_{\parallel}\right]}\left(0; \mathbf{g}_{\parallel}, E, V_{0(j+1)}, V'\right) & \mathbf{B}'_{j+1\left[\mathbf{g}_{\parallel}\right]}\left(0; \mathbf{g}_{\parallel}, E, V_{0(j+1)}, V'\right) \end{bmatrix}^{-1}$$
$$\times \begin{bmatrix} \mathbf{X}^{(\mathrm{SPC|QDL})}_{1(j+1,\,j)\left[\mathbf{g}_{\parallel}\right]} & \mathbf{0} \\ \mathbf{0} & \mathbf{X}^{(\mathrm{SPC|QDL})}_{2(j+1,\,j)\left[\mathbf{g}_{\parallel}\right]} \end{bmatrix} \begin{bmatrix} \boldsymbol{\Theta}_{j\left[\mathbf{g}_{\parallel}\right]} & \mathbf{0} \\ \mathbf{0} & \boldsymbol{\Theta}_{j\left[\mathbf{g}_{\parallel}\right]} \end{bmatrix}$$
$$\times \begin{bmatrix} \mathbf{I} & \mathbf{0} \\ \mathbf{0} & i\boldsymbol{\Xi}_{j\left[\mathbf{g}_{\parallel}\right]} \end{bmatrix} \begin{bmatrix} \mathbf{I} & \mathbf{I} \\ \mathbf{I} & -\mathbf{I} \end{bmatrix} \begin{bmatrix} \exp\left(i\boldsymbol{\Xi}_j l_j\right) & \mathbf{0} \\ \mathbf{0} & \exp\left(-i\boldsymbol{\Xi}_j l_j\right) \end{bmatrix} \tag{5.26}$$

where the matrix elements for the exchange operators $\mathbf{X}^{(\mathrm{SPC|QDL})}_{1(j+1,\,j)}$ and $\mathbf{X}^{(\mathrm{SPC|QDL})}_{2(j+1,\,j)}$ are,

$$X^{(\mathrm{SPC|QDL})}_{1(j+1,\,j)[\mathbf{g}_\parallel]lm,n} = \hat{u}_{j,n\mathbf{g}_\parallel,lm}, \tag{5.27}$$

$$X^{(\mathrm{SPC|QDL})}_{2(j+1,\,j)[\mathbf{g}_\parallel]lm,n} = \left(\hat{\mathbf{m}}^{(\mathrm{SPC|QDL})}_{(j+1,\,j)} \odot \hat{\mathbf{u}}_{j,n\mathbf{g}_\parallel}\right)_{lm}, \tag{5.28}$$

$$m^{(\mathrm{SPC|QDL})}_{(j+1,\,j)}\left(\mathbf{r}_\parallel\right) = \frac{m^{(\mathrm{SPC})}_{j+1}}{m^{(\mathrm{QDL})}_{j}\left(\mathbf{r}_\parallel\right)}, \tag{5.29}$$

and $\hat{\mathbf{m}}^{(\mathrm{SPC|QDL})}_{(j+1,\,j)}$ denotes the vector of Fourier-series coefficients for the periodic ratio-of-effective-masses function $m^{(\mathrm{SPC|QDL})}_{(j+1,\,j)}\left(\mathbf{r}_\parallel\right)$.

5.3. Contact-QDL coupling . This case must be considered when a QDL is grown directly on the bottom contact layer, or when the top contact layer is grown immediate above a QDL. The lateral basis functions are identical in the contact and spacer regions. Therefore, the coupling patterns derived in Section 5.2 also apply to this case.

THEOREM 5.10. *At the interface between a contact and a QDL, for each $\mathbf{g}_\parallel \in \mho_\parallel$, coupling occurs only between contact modes with lateral behavior $\left|\mathbf{g}_{\parallel lm}\right\rangle = \left|\mathbf{g}_\parallel + \mathbf{G}_{\parallel lm}\right\rangle$, $(l,m) \in \mathbb{Z}^2$, and QDL modes with lateral behavior $\left|n\mathbf{g}_\parallel\right\rangle$, $n \in \mathbb{N}$. There is no coupling between contact modes with lateral behavior $\left|\mathbf{g}_{\parallel lm}\right\rangle$ and QDL modes with lateral behavior $\left|n\mathbf{g}'_\parallel\right\rangle$, for all $n \in \mathbb{N}$, $(l,m) \in \mathbb{Z}^2$, when $\mathbf{g}_\parallel \neq \mathbf{g}'_\parallel$.*

COROLLARY 5.11. *The BZV-subspaces $\mathcal{F}_{[\mathbf{g}_\parallel]} \otimes \mathbb{C}^2$, $\mathbf{g}_\parallel \in \mho_\parallel$, are irreducible invariant subspaces for the local T-operators $\mathbf{T}^{(QDL|INJ)}_{(1,\,0)}$ and $\mathbf{T}^{(TRA|QDL)}_{(J+1,\,J)}$. These operators are the direct sum of their restrictions to all BZV-subspaces and are block-diagonal in natural ordering of eigenbases in both regions resulting from the imposition of the same total order $<$ on $\mho_\parallel$.*

$$\mathbf{T}^{(QDL|INJ)}_{(1,\,0)} \equiv \bigoplus_{\mathbf{g}_\parallel \in \mho_\parallel} \mathbf{T}^{(QDL|INJ)}_{(1,\,0)[\mathbf{g}_\parallel]}, \tag{5.30}$$

$$\mathbf{T}^{(TRA|QDL)}_{(J+1,\,J)} \equiv \bigoplus_{\mathbf{g}_\parallel \in \mho_\parallel} \mathbf{T}^{(TRA|QDL)}_{(J+1,\,J)[\mathbf{g}_\parallel]}. \tag{5.31}$$

5.3.1. Injecting-contact-to-QDL coupling. The restricted transfer matrix for this case is, with component-major basis-ordering,

$$\begin{bmatrix} \mathbf{a}^{(\mathrm{QDL})}_{1[\mathbf{g}_\parallel]} \\ \mathbf{b}^{(\mathrm{QDL})}_{1[\mathbf{g}_\parallel]} \end{bmatrix} = \mathbf{T}^{(\mathrm{QDL|INJ})}_{(1,0)[\mathbf{g}_\parallel]} \begin{bmatrix} \mathbf{a}^{(\mathrm{INJ})}_{0[\mathbf{g}_\parallel]} \\ \mathbf{b}^{(\mathrm{INJ})}_{0[\mathbf{g}_\parallel]} \end{bmatrix}, \tag{5.32}$$

$$\begin{aligned} \mathbf{T}^{(\mathrm{QDL|INJ})}_{(1,0)[\mathbf{g}_\parallel]} = \frac{1}{2} \begin{bmatrix} \mathbf{I} & \mathbf{I} \\ \mathbf{I} & -\mathbf{I} \end{bmatrix} \begin{bmatrix} \mathbf{I} & \mathbf{0} \\ \mathbf{0} & \mathbf{\Xi}^{-1}_{1[\mathbf{g}_\parallel]} \end{bmatrix} \begin{bmatrix} \mathbf{\Theta}^{-1}_{1[\mathbf{g}_\parallel]} & \mathbf{0} \\ \mathbf{0} & \mathbf{\Theta}^{-1}_{1[\mathbf{g}_\parallel]} \end{bmatrix} \\ \times \begin{bmatrix} \mathbf{X}^{(\mathrm{QDL|INJ})}_{1(1,0)[\mathbf{g}_\parallel]} & \mathbf{0} \\ \mathbf{0} & \mathbf{X}^{(\mathrm{QDL|INJ})}_{2(1,0)[\mathbf{g}_\parallel]} \end{bmatrix} \begin{bmatrix} 1 & 0 \\ 0 & \mathbf{K}^{(\mathrm{INJ})}_{z[\mathbf{g}_\parallel]} \end{bmatrix} \begin{bmatrix} \mathbf{I} & \mathbf{I} \\ \mathbf{I} & -\mathbf{I} \end{bmatrix} \end{aligned} \tag{5.33}$$

where the matrix elements for the exchange operators $\mathbf{X}^{(\mathrm{QDL|INJ})}_{1(1,0)\left[\mathbf{g}_\parallel\right]}$ and $\mathbf{X}^{(\mathrm{QDL|INJ})}_{2(1,0)\left[\mathbf{g}_\parallel\right]}$ are,

$$X^{(\mathrm{QDL|INJ})}_{1(1,0)\left[\mathbf{g}_\parallel\right]\,n,lm} = \hat{u}^{*}_{1,n\mathbf{g}_\parallel,lm}, \tag{5.34}$$

$$X^{(\mathrm{QDL|INJ})}_{2(1,0)\left[\mathbf{g}_\parallel\right]\,n,lm} = \left(\hat{\mathbf{u}}^{*}_{1,n\mathbf{g}_\parallel} \odot \hat{\mathbf{m}}^{(\mathrm{QDL|INJ})}_{(1,0)}\right)_{lm}, \tag{5.35}$$

$$m^{(\mathrm{QDL|INJ})}_{(1,0)}\left(\mathbf{r}_\parallel\right) = \frac{m^{(\mathrm{QDL})}_{1}\left(\mathbf{r}_\parallel\right)}{m^{(\mathrm{INJ})}}, \tag{5.36}$$

where $\hat{\mathbf{m}}^{(\mathrm{QDL|INJ})}_{(1,0)}$ is the vector of Fourier-series coefficients for the periodic effective-mass-ratio function. The $\mathbf{K}^{(\mathrm{INJ})}_{z\left[\mathbf{g}_\parallel\right]}$ operator in Eqn. (5.33) has diagonal matrix representation,

$$K^{(\mathrm{INJ})}_{z\left[\mathbf{g}_\parallel\right]lm,lm} = \sqrt{\frac{2m^{(\mathrm{INJ})}\left(E - V^{(\mathrm{INJ})}\right)}{\hbar^2} - \left\|\mathbf{g}_{\parallel lm}\right\|^2}. \tag{5.37}$$

5.3.2. QDL-to-transmitting-contact coupling. The expression for the restricted local transfer matrix is, with component-major basis-ordering,

$$\begin{bmatrix} \mathbf{a}^{(\mathrm{TRA})}_{J+1\left[\mathbf{g}_\parallel\right]} \\ \mathbf{b}^{(\mathrm{TRA})}_{J+1\left[\mathbf{g}_\parallel\right]} \end{bmatrix} = \mathbf{T}^{(\mathrm{TRA|QDL})}_{(J+1,\,J)\left[\mathbf{g}_\parallel\right]} \begin{bmatrix} \mathbf{a}^{(\mathrm{QDL})}_{J\left[\mathbf{g}_\parallel\right]} \\ \mathbf{b}^{(\mathrm{QDL})}_{J\left[\mathbf{g}_\parallel\right]} \end{bmatrix}, \tag{5.38}$$

$$\begin{aligned} \mathbf{T}^{(\mathrm{TRA|QDL})}_{(J+1,\,J)\left[\mathbf{g}_\parallel\right]} = \frac{1}{2} \begin{bmatrix} \mathbf{I} & \mathbf{I} \\ \mathbf{I} & -\mathbf{I} \end{bmatrix} &\begin{bmatrix} 1 & 0 \\ 0 & \left(\mathbf{K}^{(\mathrm{TRA})}_{z\left[\mathbf{g}_\parallel\right]}\right)^{-1} \end{bmatrix} \begin{bmatrix} \mathbf{X}^{(\mathrm{TRA|QDL})}_{1(J+1,\,J)\left[\mathbf{g}_\parallel\right]} & \mathbf{0} \\ \mathbf{0} & \mathbf{X}^{(\mathrm{TRA|QDL})}_{2(J+1,\,J)\left[\mathbf{g}_\parallel\right]} \end{bmatrix} \\ &\times \begin{bmatrix} \mathbf{\Theta}_{J\left[\mathbf{g}_\parallel\right]} & \mathbf{0} \\ \mathbf{0} & \mathbf{\Theta}_{J\left[\mathbf{g}_\parallel\right]} \end{bmatrix} \begin{bmatrix} \mathbf{I} & \mathbf{0} \\ \mathbf{0} & \mathbf{\Xi}_{J\left[\mathbf{g}_\parallel\right]} \end{bmatrix} \begin{bmatrix} \mathbf{I} & \mathbf{I} \\ \mathbf{I} & -\mathbf{I} \end{bmatrix} \\ &\times \begin{bmatrix} \exp\left(i\mathbf{\Xi}_J l_J\right) & \mathbf{0} \\ \mathbf{0} & \exp\left(-i\mathbf{\Xi}_J l_J\right) \end{bmatrix} \end{aligned} \tag{5.39}$$

where the matrix elements for the exchange operators $\mathbf{X}^{(\mathrm{TRA|QDL})}_{1(J+1,\,J)\left[\mathbf{g}_\parallel\right]}$ and $\mathbf{X}^{(\mathrm{TRA|QDL})}_{2(J+1,\,J)\left[\mathbf{g}_\parallel\right]}$ are,

$$X^{(\mathrm{TRA|QDL})}_{1(J+1,\,J)\left[\mathbf{g}_\parallel\right]\,lm,n} = \hat{u}_{J,n\mathbf{g}_\parallel,lm}, \tag{5.40}$$

$$X^{(\mathrm{TRA|QDL})}_{2(J+1,\,J)\left[\mathbf{g}_\parallel\right]\,lm,n} = \left(\hat{\mathbf{m}}^{(\mathrm{TRA|QDL})}_{(J+1,\,J)} \odot \hat{\mathbf{u}}_{J,n\mathbf{g}_\parallel}\right)_{lm}, \tag{5.41}$$

$$m^{(\mathrm{TRA|QDL})}_{(J+1,\,J)}\left(\mathbf{r}_\parallel\right) = \frac{m^{(\mathrm{TRA})}}{m^{(\mathrm{QDL})}_{J}\left(\mathbf{r}_\parallel\right)}, \tag{5.42}$$

where $\hat{\mathbf{m}}^{(\mathrm{TRA|QDL})}_{(J+1,\,J)}$ is the vector of Fourier-series coefficients for the periodic effective-mass-ratio function. The $\mathbf{K}^{(\mathrm{TRA})}_{z\left[\mathbf{g}_\parallel\right]}$ operator in Eqn. (5.39) has diagonal matrix representation,

$$K^{(\mathrm{TRA})}_{z\left[\mathbf{g}_\parallel\right]lm,lm} = \sqrt{\frac{2m^{(\mathrm{TRA})}\left(E - V^{(\mathrm{TRA})}\right)}{\hbar^2} - \left\|\mathbf{g}_{\parallel lm}\right\|^2}. \tag{5.43}$$

5.4. Inter-spacer coupling . Following the general T-matrix derivation procedure, we find that the effective-mass-ratio function in Eqn. (5.7) is constant. Therefore, the exchange expressions in both Eqn. (5.6) and Eqn. (5.7) reduce to the product of a constant and the inner product between lateral modes. From Eqn. (4.8), we note that the lateral behavior in these regions is of the form $\left|\mathbf{k}_\parallel\right\rangle_j$ and $\left|\mathbf{k'}_\parallel\right\rangle_{j+1}$, $\mathbf{k}_\parallel, \mathbf{k'}_\parallel \in \mathbb{R}^2$. Because of orthonormality, $\left\langle\mathbf{k'}_\parallel \mid \mathbf{k}_\parallel\right\rangle = \left\langle\mathbf{k}_\parallel \mid \mathbf{k'}_\parallel\right\rangle = \delta\left(\mathbf{k}_\parallel - \mathbf{k'}_\parallel\right)$, inter-mode coupling is non-zero only when lateral behavior is identical and this proves the following theorem.

THEOREM 5.12. *At the interface between two spacers with region-indices j and $j+1$, for each $\mathbf{k}_\parallel \in \mathbb{K}$, modes $\left|\mathbf{k}_\parallel\right\rangle_j$ and $\left|\mathbf{k}_\parallel\right\rangle_{j+1}$ couple only with each other. For any $\mathbf{k'}_\parallel \in \mathbb{K}$, coupling between modes $\left|\mathbf{k}_\parallel\right\rangle_j$ and $\left|\mathbf{k'}_\parallel\right\rangle_{j+1}$ is zero if $\mathbf{k}_\parallel \neq \mathbf{k'}_\parallel$.*

COROLLARY 5.13. *The local transfer operator is the direct sum of its restrictions to all $\mathcal{F}_{\mathbf{k}_\parallel} \otimes \mathbb{C}^2$, $\mathbf{k}_\parallel \in \mathbb{K}$. The T-matrix is block-diagonal, with 2×2 blocks, in a mode-major ordering of the bases and can therefore be expressed as a 2×2 block-partitioned matrix, with diagonal blocks, in a component-major ordering of the bases.*

$$\mathbf{T}^{(SPC|SPC)}_{(j+1,\,j)} \equiv \bigoplus_{\mathbf{k}_\parallel \in \mathbb{K}} \mathbf{T}^{(SPC|SPC)}_{(j+1,\,j)\left[\mathbf{k}_\parallel\right]}. \tag{5.44}$$

Substituting Eqn. (4.8) into both sides of Eqn. (5.3) and Eqn. (5.4), projecting onto various $\left|\mathbf{k}_\parallel\right\rangle$, and grouping the results we get,

$$\begin{bmatrix} a^{(\mathrm{SPC})}_{j+1}\left(\mathbf{k}_\parallel\right) \\ b^{(\mathrm{SPC})}_{j+1}\left(\mathbf{k}_\parallel\right) \end{bmatrix} \stackrel{\mathrm{def}}{=} \mathbf{T}^{(\mathrm{SPC|SPC})}_{(j+1,j)\left[\mathbf{k}_\parallel\right]} \begin{bmatrix} a^{(\mathrm{SPC})}_{j}\left(\mathbf{k}_\parallel\right) \\ b^{(\mathrm{SPC})}_{j}\left(\mathbf{k}_\parallel\right) \end{bmatrix}, \tag{5.45}$$

$$\begin{aligned} \mathbf{T}^{(\mathrm{SPC|SPC})}_{(j+1,\,j)\left[\mathbf{k}_\parallel\right]} = {} & \begin{bmatrix} \mathrm{Ai}\left(\sigma\left(0;\mathbf{k}_\parallel, E, V_{0(j+1)}, V'\right)\right) & \mathrm{Bi}\left(\sigma\left(0;\mathbf{k}_\parallel, E, V_{0(j+1)}, V'\right)\right) \\ \mathrm{Ai}'\left(\sigma\left(0;\mathbf{k}_\parallel, E, V_{0(j+1)}, V'\right)\right) & \mathrm{Bi}'\left(\sigma\left(0;\mathbf{k}_\parallel, E, V_{0(j+1)}, V'\right)\right) \end{bmatrix}^{-1} \\ & \times \begin{bmatrix} 1 & 0 \\ 0 & \frac{m^{(\mathrm{SPC})}_{(j+1)}}{m^{(\mathrm{SPC})}_{j}} \end{bmatrix} \\ & \times \begin{bmatrix} \mathrm{Ai}\left(\sigma\left(l_j;\mathbf{k}_\parallel, E, V_{0j}, V'\right)\right) & \mathrm{Bi}\left(\sigma\left(l_j;\mathbf{k}_\parallel, E, V_{0j}, V'\right)\right) \\ \mathrm{Ai}'\left(\sigma\left(l_j;\mathbf{k}_\parallel, E, V_{0j}, V'\right)\right) & \mathrm{Bi}'\left(\sigma\left(l_j;\mathbf{k}_\parallel, E, V_{0j}, V'\right)\right) \end{bmatrix} \end{aligned} \tag{5.46}$$

5.5. Spacer-contact coupling . The lateral behavior of modes in both contact and spacer regions (Eqn. (4.2) and Eqn. (4.8)) is of planewave form $\left\{\left|\mathbf{k}_\parallel\right\rangle \mid \mathbf{k}_\parallel \in \mathbb{R}^2\right\}$. As with inter-spacer coupling, because of orthonormality, $\langle\mathbf{k'}_\parallel \mid \mathbf{k}_\parallel\rangle = \delta\left(\mathbf{k}_\parallel - \mathbf{k'}_\parallel\right)$, coupling is non-zero only between modes whose lateral behavior is identical.

THEOREM 5.14. *At the interface between a contact and a spacer with region-indices j and $j' = j \pm 1$, for each $\mathbf{k}_\parallel \in \mathbb{K}$, modes $\left|\mathbf{k}_\parallel\right\rangle_j$ and $\left|\mathbf{k}_\parallel\right\rangle_{j'}$ couple only with each other. For any $\mathbf{k'}_\parallel \in \mathbb{K}$, coupling between modes $\left|\mathbf{k}_\parallel\right\rangle_j$ and $\left|\mathbf{k'}_\parallel\right\rangle_{j'}$ is zero if $\mathbf{k}_\parallel \neq \mathbf{k'}_\parallel$.*

COROLLARY 5.15. *The local transfer operator is the direct sum of its restrictions to all $\mathcal{F}_{\mathbf{k}_\parallel} \otimes \mathbb{C}^2$, $\mathbf{k}_\parallel \in \mathbb{K}$. The T-matrix is block-diagonal, with 2×2 blocks, in a mode-major ordering of the bases and can therefore be expressed as a 2×2 block-partitioned matrix, with diagonal blocks, in a component-major ordering of the bases.*

$$\mathbf{T}^{\textit{(SPC|INJ)}}_{(1,\,0)} \equiv \bigoplus_{\mathbf{k}_\parallel \in \mathbb{K}} \mathbf{T}^{\textit{(SPC|INJ)}}_{(1,\,0)\left[\mathbf{k}_\parallel\right]}, \tag{5.47}$$

$$\mathbf{T}^{\textit{(TRA|SPC)}}_{(J+1,\,J)} \equiv \bigoplus_{\mathbf{k}_\parallel \in \mathbb{K}} \mathbf{T}^{\textit{(TRA|SPC)}}_{(J+1,\,J)\left[\mathbf{k}_\parallel\right]}. \tag{5.48}$$

Following the general procedure for establishing the T-matrix and using Eqn. (4.2) and Eqn. (4.8) for the wavefunctions, coupling from the injecting contact to the following spacer region is given by,

$$\left[\begin{array}{c} a_1^{(\mathrm{SPC})}\left(\mathbf{k}_\parallel\right) \\ b_1^{(\mathrm{SPC})}\left(\mathbf{k}_\parallel\right) \end{array}\right] \stackrel{\mathrm{def}}{=} \mathbf{T}^{(\mathrm{SPC|INJ})}_{(1,\,0)\left[\mathbf{k}_\parallel\right]} \left[\begin{array}{c} a_0^{(\mathrm{INJ})}\left(\mathbf{k}_\parallel\right) \\ b_0^{(\mathrm{INJ})}\left(\mathbf{k}_\parallel\right) \end{array}\right], \tag{5.49}$$

$$\begin{aligned} \mathbf{T}^{(\mathrm{SPC|INJ})}_{(1,\,0)\left[\mathbf{k}_\parallel\right]} &= \left[\begin{array}{cc} \mathrm{Ai}\left(\sigma\left(0;\mathbf{k}_\parallel,E,0,V'\right)\right) & \mathrm{Bi}\left(\sigma\left(0;\mathbf{k}_\parallel,E,0,V'\right)\right) \\ \mathrm{Ai}'\left(\sigma\left(0;\mathbf{k}_\parallel,E,0,V'\right)\right) & \mathrm{Bi}'\left(\sigma\left(0;\mathbf{k}_\parallel,E,0,V'\right)\right) \end{array}\right]^{-1} \\ &\times \left[\begin{array}{cc} 1 & 0 \\ 0 & i\frac{m_1^{(\mathrm{SPC})}}{m^{(\mathrm{INJ})}} k_z^{(\mathrm{INJ})}\left(E,\mathbf{k}_\parallel\right) \end{array}\right] \left[\begin{array}{cc} 1 & 1 \\ 1 & -1 \end{array}\right]. \end{aligned} \tag{5.50}$$

The local transfer matrix for coupling to the transmitting contact from a spacer that happens to immediately precede it can be expressed as, for arbitrary $\mathbf{k}_\parallel \in \mathbb{K}$,

$$\left[\begin{array}{c} a_{J+1}^{(\mathrm{TRA})}\left(\mathbf{k}_\parallel\right) \\ b_{J+1}^{(\mathrm{TRA})}\left(\mathbf{k}_\parallel\right) \end{array}\right] \stackrel{\mathrm{def}}{=} \mathbf{T}^{(\mathrm{TRA|SPC})}_{(J+1,\,J)\left[\mathbf{k}_\parallel\right]} \left[\begin{array}{c} a_J^{(\mathrm{SPC})}\left(\mathbf{k}_\parallel\right) \\ b_J^{(\mathrm{SPC})}\left(\mathbf{k}_\parallel\right) \end{array}\right], \tag{5.51}$$

$$\begin{aligned} \mathbf{T}^{(\mathrm{TRA|SPC})}_{(J+1,\,J)\left[\mathbf{k}_\parallel\right]} &= \frac{1}{2}\left[\begin{array}{cc} 1 & 1 \\ 1 & -1 \end{array}\right] \left[\begin{array}{cc} 1 & 0 \\ 0 & -i\frac{m^{(\mathrm{TRA})}}{m_J^{(\mathrm{SPC})}} \times \frac{1}{k_z^{(\mathrm{TRA})}\left(E,\mathbf{k}_\parallel\right)} \end{array}\right] \\ &\times \left[\begin{array}{cc} \mathrm{Ai}\left(\sigma\left(l_J;\mathbf{k}_\parallel,E,V_{0J},V'\right)\right) & \mathrm{Bi}\left(\sigma\left(l_J;\mathbf{k}_\parallel,E,V_{0J},V'\right)\right) \\ \mathrm{Ai}'\left(\sigma\left(l_J;\mathbf{k}_\parallel,E,V_{0J},V'\right)\right) & \mathrm{Bi}'\left(\sigma\left(l_J;\mathbf{k}_\parallel,E,V_{0J},V'\right)\right) \end{array}\right]. \end{aligned} \tag{5.52}$$

5.6. Global Transfer Matrix . The global transfer operator for the device is the composition of local transfer operators according to the sequence of interfaces from the injecting to the transmitting contact and relates the amplitudes of the incident and reflected components at the transmitting contact to those at the incident contact. In component-major basis order, the global T-matrix is,

$$\left[\begin{array}{c} \mathbf{a}_{J+1}^{(\mathrm{TRA})} \\ \mathbf{b}_{J+1}^{(\mathrm{TRA})} \end{array}\right] \stackrel{\mathrm{def}}{=} \mathbf{T}^{(\mathrm{TRA|INJ})}_{J+1,0} \left[\begin{array}{c} \mathbf{a}_0^{(\mathrm{INJ})} \\ \mathbf{b}_0^{(\mathrm{INJ})} \end{array}\right], \tag{5.53}$$

$$\mathbf{T}^{(\mathrm{TRA|INJ})}_{J+1,0} \equiv \mathbf{T}_{(J+1,\,J)}\mathbf{T}_{(J,\,J-1)}\ldots\mathbf{T}_{(2,1)}\mathbf{T}_{(1,0)}. \tag{5.54}$$

Each type of local transfer operator that can occur in the chain is expressible as the direct sum of its restrictions to a specific set of irreducible invariant subspaces. Because spacer and contact regions can be tiled into repeating unit-cell areas, their

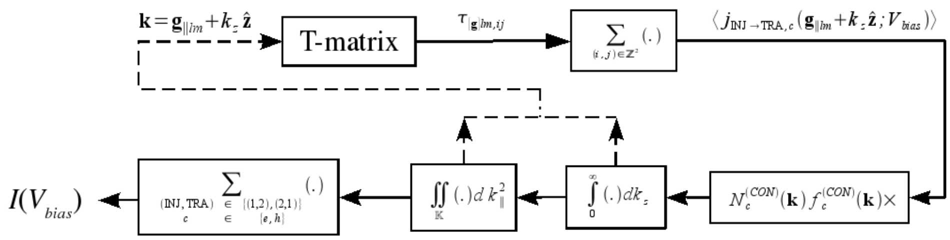

FIGURE 6.1. *Flowchart depicting the current calculation process*

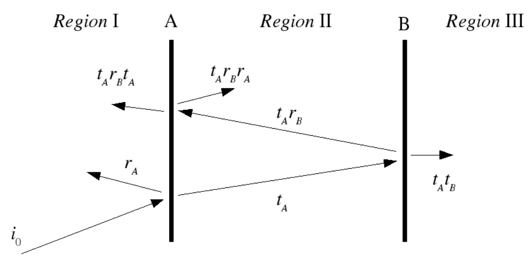

FIGURE 6.2. *Schematic depiction of multiple sequential scattering of an incident mode from different interfaces in the device. Each mode incident on an interface gives rise to a reflected component and a transmitted component. These are again incident on other interfaces. Scattering occurs ad-infinitum.*

irreducible $\mathcal{F}_{\mathbf{k}_\parallel}$-subspaces give rise to their $\mathcal{F}_{[\mathbf{g}_\parallel]}$ subspaces through an external direct-sum. Therefore, the various $\mathcal{F}_{[\mathbf{g}_\parallel]}$ are the smallest invariant subspaces common to all regions in the device. The following theorem formalizes this notion.

THEOREM 5.16. *The global T-operator is the direct sum of its restrictions to all BZV-subspaces.*

Proof. From corollary 5.7, corollary 5.9, and corollary 5.11 we note that the various BZV-subspaces, $\mathcal{F}_{[\mathbf{g}_\parallel]} \otimes \mathbb{C}^2 \quad \left(\mathbf{g}_\parallel \in \mho_\parallel\right)$, form (irreducible) invariant subspaces for the local T-operators corresponding to interfaces where at least one region is a QDL slice. From corollary 5.13 and corollary 5.15 we note that the various $\mathcal{F}_{\mathbf{k}_\parallel} \otimes \mathbb{C}^2 \quad \left(\mathbf{k}_\parallel \in \mathbb{K}\right)$ form irreducible invariant-subspaces for the local T-operators corresponding to interfaces where both regions are homogeneous (spacers or contacts). From the group-theoretic facts in Appendix A, $\mathcal{F}_{[\mathbf{g}_\parallel]} \otimes \mathbb{C}^2 = \bigoplus_{(l,m)\in\mathbb{Z}^2} \mathcal{F}_{\mathbf{g}_{\parallel lm}} \otimes \mathbb{C}^2$. Therefore all BZV-subspaces are exhaustive, invariant-subspaces for all types of local T-operators. They are therefore exhaustive, invariant-subspaces for the global T-operator also, which just the composition of a sequence of local T-operators. QED. □

It therefore suffices to work with the expression for the restriction of the global T-operator to an arbitrary BZV-subspace,

$$\begin{bmatrix} \mathbf{a}^{(\mathrm{TRA})}_{J+1[\mathbf{g}_\parallel]} \\ \mathbf{b}^{(\mathrm{TRA})}_{J+1[\mathbf{g}_\parallel]} \end{bmatrix} \stackrel{\mathrm{def}}{=} \mathbf{T}^{(\mathrm{TRA}|\mathrm{INJ})}_{J+1,0[\mathbf{g}_\parallel]} \begin{bmatrix} \mathbf{a}^{(\mathrm{INJ})}_{0[\mathbf{g}_\parallel]} \\ \mathbf{b}^{(\mathrm{INJ})}_{0[\mathbf{g}_\parallel]} \end{bmatrix}, \tag{5.55}$$

$$\mathbf{T}^{(\mathrm{TRA}|\mathrm{INJ})}_{J+1,0[\mathbf{g}_\parallel]} = \mathbf{T}_{J+1,\,J[\mathbf{g}_\parallel]} \mathbf{T}_{J,\,J-1[\mathbf{g}_\parallel]} \cdots \mathbf{T}_{1,0[\mathbf{g}_\parallel]}. \tag{5.56}$$

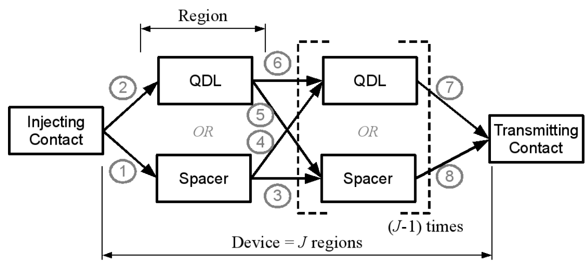

FIGURE 6.3. *Schematic depiction of the composition of the local T-matrices to form the global T-matrix. Numeric labels indicate specific local T-matrices:* (1) $\mathbf{T}^{(SPC|INJ)}_{(1,0)}$ (2) $\mathbf{T}^{(QDL|INJ)}_{(1,0)}$ (3) $\mathbf{T}^{(SPC|SPC)}_{(j+1,\,j)}$ (4) $\mathbf{T}^{(SPC|QDL)}_{(j+1,\,j)}$ (5) $\mathbf{T}^{(QDL|SPC)}_{(j+1,\,j)}$ (6) $\mathbf{T}^{(QDL|QDL)}_{(j+1,\,j)}$ (7) $\mathbf{T}^{(TRA|QDL)}_{(J+1,\,J)}$ (8) $\mathbf{T}^{(TRA|SPC)}_{(J+1,\,J)}$.

6. Current calculation . Figure 6.1 depicts the current calculation process as described earlier in the general formalism (Section 3). The global T-matrix captures the ad-infinitum multiple sequential scattering of the incident, reflected and transmitted waves at all interfaces (schematically depicted in figure 6.2) brought about by the the incident phase at the injecting contact. Figure 6.3 shows the types of local T-matrices whose composition forms the global T-matrix. From the structure of the local T-operators, we observe that at any interface, an incident component with lateral behavior $\left|\mathbf{g}_\parallel + \mathbf{G}_{\parallel lm}\right\rangle$, for some $(l,m) \in \mathbb{Z}^2$, is scattered into reflected and transmitted components within the same BZV-subspace, $\mathcal{F}_{\left[\mathbf{g}_\parallel\right]}$. These modes, in turn, are forward- and back-scattered within the same BZV-subspace at every subsequent scattering event. This property of lateral-mode scattering within the same BZV-subspace holds for all T-operators regardless of their number and position-of-evaluation. In limit, this property holds continuously throughout the growth-direction - because the entire device shares the same lateral Brillouin zone by design, each incident phase is diffracted into a combination of planewaves with regularly-spaced wavevectors.

COROLLARY 6.1. *An incident mode with lateral behavior* $\left|\mathbf{g}_\parallel + \mathbf{G}_{\parallel lm}\right\rangle$, $\mathbf{g}_\parallel \in \mho_\parallel$, $(l,m) \in \mathbb{Z}^2$ *couples only with the following types of modes:*

1. all modes that laterally behave as $\left|\mathbf{g}_\parallel + \mathbf{G}_{\parallel ij}\right\rangle$, $(i,j) \in \mathbb{Z}^2$, in the incident contact (reflected wavefunction), spacer regions and transmitting contact (transmitted wavefunction), and
2. modes with lateral behavior $\left|n\mathbf{g}_\parallel\right\rangle$, all $n \in \mathbb{N}$, in QDL slices.

Because the lateral behavior of every incident mode is expressible as the sum of some Brillouin zone vector and some reciprocal-lattice vector, this Brillouin zone vector dictates the BZV-subspace inside which all calculations can be completely performed. Due to this, the continuous distribution of the reflected and transmitted wavefunctions over iso-energy wavevectors in Eqn. (3.9) and Eqn. (3.10) for an arbitrary incident $\mathbf{k}^{(\mathrm{INC})} = \mathbf{g}_{\parallel lm} + k_z\hat{\mathbf{z}}$, $E = E^{(\mathrm{INJ})}\left(\mathbf{k}^{(\mathrm{INC})}\right)$ must be recast as discrete sums,

$$(6.1)\quad \Psi^{(\mathrm{REFL})}\left(\mathbf{r};\mathbf{g}_{\parallel lm} + k_z\hat{\mathbf{z}}\right) \equiv \sum_{(l',m')\in\mathbb{Z}^2} \rho_{\left[\mathbf{g}_\parallel\right]lm,l'm'}\left(k_z\right) \times \exp\left[i\left(\mathbf{g}_{\parallel l'm'} - k_z^{(\mathrm{INJ})}\left(E,\mathbf{g}_{\parallel \mathbf{l'm'}_\parallel}\right)\hat{\mathbf{z}}\right)\bullet\mathbf{r}\right],$$

$$(6.2)\quad \rho_{\left[\mathbf{g}_\parallel\right]lm,l'm'}\left(k_z\right) \stackrel{\mathrm{def}}{=} \rho\left(\mathbf{g}_{\parallel lm} + k_z\hat{\mathbf{z}},\, \mathbf{g}_{\parallel l'm'} - k_z^{(\mathrm{INJ})}\left(E,\mathbf{g}_{\parallel l'm'}\right)\hat{\mathbf{z}}\right),$$

$$(6.3)\quad \Psi^{(\mathrm{TRA})}\left(\mathbf{r};\mathbf{g}_{\parallel lm} + k_z\hat{\mathbf{z}}\right) \equiv \sum_{(l',m')\in\mathbb{Z}^2} \tau_{\left[\mathbf{g}_\parallel\right]lm,l'm'}\left(k_z\right) \times$$

$$\exp\left[i\left(\mathbf{g}_{\| l'm'} + k_z^{(\text{TRA})}\left(E, \mathbf{g}_{\|\mathbf{l'm'}_\|}\right)\hat{\mathbf{z}}\right)\bullet\mathbf{r}\right],$$

$$\tau_{[\mathbf{g}_\|]lm,l'm'}(k_z) \stackrel{\text{def}}{=} \tau\left(\mathbf{g}_{\| lm} + k_z\hat{\mathbf{z}},\, \mathbf{g}_{\| l'm'} + k_z^{(\text{TRA})}\left(E, \mathbf{g}_{\| l'm'}\right)\hat{\mathbf{z}}\right), \tag{6.4}$$

The expression for the average transmitted-probability-flux in Eqn. (3.5) now becomes,

$$\left\langle \mathrm{j}\left(\mathbf{r}_\|; \mathbf{g}_{\| lm} + k_z^{(\text{INC})}\hat{\mathbf{z}}, V_{bias}\right)\right\rangle = \sum_{(l',m')\in\mathbb{Z}^2} \left|\tau_{[\mathbf{g}_\|]lm,l'm'}(k_z)\right|^2 \times \mathrm{Re}\left\{k_z^{(\text{TRA})}\left(E, \mathbf{g}_{\| l'm'}\right)\right\}. \tag{6.5}$$

Though the summation is conceptually performed over a countably-infinite set of indices, in practice the real part of the transmitted wavevector in the above expression will be non-zero only for a finite number propagating modes in the transmitting contact - other modes will be either evanescent ($k_z \in i\mathbb{R}^+$) or unphysical ($k_z \in i\mathbb{R}^-$). Evanescent modes do not contribute to probability-current and unphysical modes must not be considered as part of the general solution for the wavefunction.

7. Conclusions and future work. We have derived the diffraction pattern for charge-carrier wavefunctions through layers of quantum dots stacked between two ohmic contacts under different conditions of externally-applied voltage. All quantum dots within a QDL are identical and show perfect lateral Bravais lattice arrangement within the layer. All layers are perfectly aligned so that the entire device as a well-defined lateral unit cell. A wealth of recent experimental work supports and motivates this study.

We have employed a single-band, effective-mass Schrödinger equation description of the wavefunction physics. The lateral symmetry justifies the use of the Bloch form for the lateral wavefunction components which naturally includes long-range, in-plane correlations between quantum dots. Out-of-plane correlations are achieved through composition of T-operators which arise at interfaces resulting from discretization along the growth direction.

We have proved that incident charge-carrier wavefunction phases are diffracted into specific patterns of propagating out-going phases and that throughout the growth direction, the distribution over lateral mode wavevectors is closed within the specific coset of the reciprocal-lattice-vector point group corresponding to the incident mode. This is true as long as the effective-mass and band profiles remain laterally periodic and we expect this to hold in a variety of model-realizations that may or may not include strain and self-consistency since mathematical descriptions of physically-plausible phenomena must maintain laterally periodicity.

A significant mathematical consequence of this diffraction pattern is that all calculations can be performed independently within a special lateral function-subspace established by the incident-wave. Computationally, this leads to greatly-increased parallelism through independence of calculations in different subspaces, and vastly-reduced memory pressure due to decreased dimensionality of each subspace.

Though our derivations employ the T-matrix approach for conceptual development, the model must numerically implemented with care. Preliminary implementations highlight intrinsic numerical challenges - in principle, any incident phase is scattered into a full set of propagating and evanescent components in the reflected and transmitted states. Therefore, basis modes and functions must be chosen to be numerically satisfactory in addition to being physically justifiable. Limiting basis-set size to allow selected modes requires caution since the T-matrix approach, and the related S-matrix approach, require the same basis-cardinality in the domain and range (i.e., successive regions) so as to permit the inversion of a (square) sub-matrix at the final stage of computing the transmission amplitudes. While large basis-size facilitates better approximation of the conceptual representation in infinite bases, it also introduces (a large number of) exponentially decaying and growing modes into the solution thereby causing or increasing instability. In addition, pedagogical idealizations to device-geometry, like a generalized Kronig-Penney model with rectangular effective-mass and PEF profiles, lead to divergent infinite sums in the convolution expressions for certain matrix elements indicating their unphysicality. Hence, the demonstration of simulation is also contingent on finding good, physically-plausible candidate functions for the potential energy and effective-mass.

Apart from these numeric challenges, the proposed model is also limited by its neglect of effects from other phenomena like spin-orbit coupling, inter-carrier correlation, interactions with other excitations like phonons, and relativistic corrections, if any.

Our current work is directed towards systematically deriving and implementing a physically- and mathematically-justified, robust numerical procedure for simulation as well as identifying good, illustrative models for device-geometries. Future work includes study of computational characteristics, the development of efficient and accurate numerics and deployments, simulation of realistic geometries, and characterization of charge-transport for various choices of structural design parameters for the device.

The general development of the model is applicable to devices with other forms of lateral symmetry provided suitable, parametric forms of the lateral eigenfunctions exists to capture the symmetry. Despite existing limitations, the development of the proposed model has helped identify advantageous traits like the lateral function-subspace-closure property discussed above which will form the foundation for any successful implementation.

Appendix A. General and frequently-used facts .

The following group-theoretic facts are used in proving several results,

The set of wavevectors $\mathbb{K} = \left\{\mathbf{k}_{\|} \,|\, \mathbf{k}_{\|} \in \mathbb{R}^2\right\}$ forms an abelian group under vector addition. Every subgroups of an abelian group is normal.

The set $\mathbb{G} = \left\{\mathbf{G}_{\|lm} \mid (l,m) \in \mathbb{Z}^2\right\}$ forms a point-group that is invariant with respect to translations by reciprocal lattice vectors. It is a subgroup of $\mathbb{K}$.

For each $\mathbf{g}_{\|} \in \mho_{\|}$, the set $\mathbb{G}_{\left[\mathbf{g}_{\|}\right]} = \left\{\mathbf{g}_{\|lm} \mid (l,m) \in \mathbb{Z}^2\right\}$ forms a coset of $\mathbb{G}$ within $\mathbb{K}$ and is an equivalence class of $\mathbf{g}_{\|}$ under the relation $\mathbf{k}_{\|1} \,\mathfrak{R}\, \mathbf{k}_{\|2}$ iff $\left(\mathbf{k}_{\|1} - \mathbf{k}_{\|2}\right) \in \mathbb{G}$, $\mathbf{k}_{\|1}, \mathbf{k}_{\|2} \in \mathbb{K}$. The set of all these cosets forms the quotient-group $\mathbb{K}/\mathbb{G} = \left\{\mathbb{G}_{\left[\mathbf{g}_{\|}\right]} \,|\, \mathbf{g}_{\|} \in \mho_{\|}\right\}$.

$$\mathcal{F} = \bigoplus\nolimits_{\mathbf{g}_{\|} \in \mho_{\|}} \mathcal{F}_{\left[\mathbf{g}_{\|}\right]} \qquad \mathcal{F} = \bigoplus\nolimits_{\mathbf{k}_{\|} \in \mathbb{K}} \mathcal{F}_{\mathbf{k}_{\|}} \qquad \mathcal{F}_{\left[\mathbf{g}_{\|}\right]} = \bigoplus\nolimits_{(l,m) \in \mathbb{Z}^2} \mathcal{F}^{\|}_{\mathbf{g}_{\|lm}}$$

Lemma A.1. *The 2D Fourier transform of a laterally periodic function,* $a\left(\mathbf{r}_{\|}\right) \equiv a\left(\mathbf{r}_{\|} + \mathbf{R}_{\|lm}\right)$, $(l,m) \in \mathbb{Z}^2$, *to the reciprocal-space variable* $\mathbf{k}_{\|}$ *is zero unless* $\mathbf{k}_{\|}$ *is a reciprocal-lattice vector, i.e.,* $\exists\,(i,j) \in \mathbb{Z}^2 \;\; \mathbf{k}_{\|} = \mathbf{G}_{\|ij}$.

Proof. $a\left(\mathbf{r}_{\|}\right)$ has 2D Fourier series representation given by Eqn. (2.3), with coefficients $\hat{a}_{lm}$, $(l,m) \in \mathbb{Z}^2$. Its 2D Fourier transform to $\mathbf{k}_\parallel$ becomes,

$$\mathfrak{F}_\parallel \left[a\left(\mathbf{r}_\parallel\right)\right]\left(\mathbf{k}_\parallel\right) \equiv \sum_{(l,m)\in\mathbb{Z}^2} \hat{a}_{lm} \times 2\pi\delta\left(\mathbf{k}_\parallel - \mathbf{G}_{\parallel lm}\right). \tag{A.1}$$

The Dirac-comb in the final expression completes the proof.□

Corollary A.2. *Given a set of laterally periodic functions* $\{a_i\left(\mathbf{r}_\parallel\right) : i = 1,2,\ldots\}$, *i.e.* $\forall (l,m) \in \mathbb{Z}^2 : a_i\left(\mathbf{r}_\parallel\right) \equiv a_i\left(\mathbf{r}_\parallel + \mathbf{R}_{\parallel lm}\right)$, *the Fourier transform of their product to the variable* $\mathbf{k}_\parallel$ *is zero unless* $\mathbf{k}_\parallel$ *is a reciprocal-lattice vector.*

Proof. Follows from lemma A.1 because the product $\mathrm{b}\left(\mathbf{r}_\parallel\right) = \prod_i a_i\left(\mathbf{r}_\parallel\right)$ is itself periodic.□

Theorem A.3. *The Fourier transform of the periodic function* $a\left(\mathbf{r}_\parallel\right) \equiv a\left(\mathbf{r}_\parallel + \mathbf{R}_{\parallel lm}\right)$, $\forall (l,m) \in \mathbb{Z}^2$ *to the reciprocal-space vector* $\left(\mathbf{g}_{\parallel 1} - \mathbf{g}_{\parallel 2}\right)$, *for any* $\mathbf{g}_{\parallel 1}, \mathbf{g}_{\parallel 2} \in \mho_\parallel$, *is zero unless* $\mathbf{g}_{\parallel 1} = \mathbf{g}_{\parallel 2}$.

Proof. From lemma A.1, the Fourier transform is zero unless $\left(\mathbf{g}_{\parallel 1} - \mathbf{g}_{\parallel 2}\right) = \mathbf{G}_{\parallel ij}$ for some $(i,j) \in \mathbb{Z}^2$. But because $\mathbf{g}_{\parallel 1}$ and $\mathbf{g}_{\parallel 2}$ lie within the first Brillouin zone, $\left(\mathbf{g}_{\parallel 1} - \mathbf{g}_{\parallel 2}\right)$ can only equal the $\mathbf{G}_{\parallel 00} = \mathbf{0}$ reciprocal lattice vector. QED.□

Corollary A.4. *Given* periodic functions $\{a_i\left(\mathbf{r}_\parallel\right) : i = 1,2,\ldots\}$ sharing the same period, *the Fourier transform of the product* $b\left(\mathbf{r}_\parallel\right) = \prod_i a_i\left(\mathbf{r}_\parallel\right)$ *to the reciprocal-space vector* $\left(\mathbf{g}_{\parallel 1} - \mathbf{g}_{\parallel 2}\right)$, *for any* $\mathbf{g}_{\parallel 1}, \mathbf{g}_{\parallel 2} \in \mho_\parallel$, *is zero unless* $\mathbf{g}_{\parallel 1} = \mathbf{g}_{\parallel 2}$.

Appendix B. Representation and properties of QDL lateral eigenfunctions .

At any fixed value of $z = z_0$, the lateral Hamiltonian is invariant with respect to translations by arbitrary real-space lattice vectors. Therefore, the Bloch theorem [1] imposes the following structure on the real-space representation of its eigenfunctions,

$$\left\langle \mathbf{r}_\parallel \mid n\mathbf{g}_\parallel(z_0)\right\rangle \stackrel{\text{def}}{=} \phi_{n\mathbf{g}_\parallel}\left(\mathbf{r}_\parallel; z_0\right) \equiv \frac{1}{2\pi} u_{n\mathbf{g}_\parallel}\left(\mathbf{r}_\parallel; z_0\right) e^{i\mathbf{g}_\parallel \bullet \mathbf{r}_\parallel}, \tag{B.1}$$

where the constant factor of $1/2\pi$ has been introduced to ensure orthonormality of lateral basis functions, and $u_{n\mathbf{g}_\parallel}\left(\mathbf{r}_\parallel; z_0\right)$ is the central-cell function which is periodic with the lateral lattice and hence has a Fourier-series representation with coefficients $\hat{u}_{n\mathbf{g}_\parallel, lm}(z_0)$, $(l,m) \in \mathbb{Z}^2$. Therefore,

$$\phi_{n\mathbf{g}_\parallel}\left(\mathbf{r}_\parallel; z_0\right) \equiv \frac{1}{2\pi} \sum_{(l,m)\in\mathbb{Z}^2} \hat{u}_{n\mathbf{g}_\parallel, lm}(z_0)\, e^{i\mathbf{g}_{\parallel lm} \bullet \mathbf{r}_\parallel}, \tag{B.2}$$

which makes the vector of coefficients $\hat{\mathbf{u}}_{n\mathbf{g}_\parallel}(z_0)$ the representation of $\left|n\mathbf{g}_\parallel(z_0)\right\rangle$ in reciprocal space. Being a linear combination exclusively of $\left|\mathbf{g}_{\parallel lm}\right\rangle$, $(l,m) \in \mathbb{Z}^2$, $\left|n\mathbf{g}_\parallel(z_0)\right\rangle$ is a vector in $\mathcal{F}_{\left[\mathbf{g}_\parallel\right]}$.

Because the lateral Hamiltonian is hermitian , these eigenfunctions are orthogonal, and normal without loss of generality,

$$\begin{aligned} \left\langle n_1\mathbf{g}_{\parallel 1}(z_0) \mid n_2\mathbf{g}_{\parallel 2}(z_0)\right\rangle &\equiv \iint_{\mathbb{R}^2} \phi^*_{n_1\mathbf{g}_{\parallel 1}}\left(\mathbf{r}_\parallel; z_0\right) \phi_{n_2\mathbf{g}_{\parallel 2}}\left(\mathbf{r}_\parallel; z_0\right) d^2 r_\parallel \\ &= \delta_{n_1 n_2}\delta\left(\mathbf{g}_{\parallel 1} - \mathbf{g}_{\parallel 2}\right), \end{aligned} \tag{B.3}$$

$$\Rightarrow \hat{\mathbf{u}}^*_{n_1\mathbf{g}_{\parallel 1}}(z_0) \bullet \hat{\mathbf{u}}_{n_2\mathbf{g}_{\parallel 2}}(z_0) \stackrel{\text{def}}{=} \sum_{(l,m)\in\mathbb{Z}^2} \hat{u}^*_{n_1\mathbf{g}_{\parallel 1}, lm}(z_0)\, \hat{u}_{n_2\mathbf{g}_{\parallel 2}, lm}(z_0) \tag{B.4}$$

$$= \begin{cases} \delta_{n_1 n_2}, & \mathbf{g}_{\|1} = \mathbf{g}_{\|2} \quad , \\ 0, & \mathbf{g}_{\|1} \neq \mathbf{g}_{\|2} \quad . \end{cases}$$

For physically-plausible Hamiltonians, the lateral eigenfunctions form a complete set,

$$\text{(B.5)} \qquad \iint_{\mho_\|} \sum_{n \in \mathbb{N}} \left| n\mathbf{g}_\| (z_0) \right\rangle \left\langle n\mathbf{g}_\| (z_0) \right| d^2 g_\| = \mathbf{I}.$$

Proposition B.1. *Given* $z = z_0$, $\forall \mathbf{g}_\| \in \mho_\|$, *the subset* $\mathbf{\Phi}_{[\mathbf{g}_\|]} = \left\{ \left| n\mathbf{g}_\| (z_0) \right\rangle \mid n \in \mathbb{N} \right\}$ *of the lateral eigenbasis generates the BZV-subspace corresponding to* $\mathbf{g}_\|$, *i.e.,*

$$span \left\{ \left| n\mathbf{g}_\| (z_0) \right\rangle \mid n \in \mathbb{N} \right\} = \mathcal{F}_{[\mathbf{g}_\|]}.$$

Proof. Follows from the fact that the lateral eigenfunctions are mutually orthonormal and form a complete set and therefore, the subset that lies within any subspace must generate that subspace. Hence $\mathbf{\Phi}_{[\mathbf{g}_\|]} (z_0)$ must form a complete, orthonormal basis for $\mathcal{F}_{[\mathbf{g}_\|]}$. □

Since the set of reciprocal-space basis states $\mathcal{G}_{[\mathbf{g}_\|]} = \left\{ \left| \mathbf{g}_{\| lm} \right\rangle \mid (l, m) \in \mathbb{Z}^2 \right\}$ also forms a complete, orthonormal basis for this BZV-subspace, both basis-subsets are equivalent, i.e., there exists a unitary transformation that maps a representation of any vector in one system to its representation in the other. Eqn. (B.2) and Eqn. (B.4) indicate that the various $\hat{u}_{n\mathbf{g}_\|, lm}$ provide the matrix elements for these transformations

Appendix C. Matrix Elements for local mode-coupling operators in vector-ODE form of TISE .

C.1. KE Operator of BenDaniel-Duke. Substituting Eqn. (4.16) into Eqn. (4.22), multiplying through by $2m_0/\hbar^2$ and rearranging, we get,

$$\text{(C.1)} \qquad \frac{\partial}{\partial z} \left\{ \mathbf{M}^{-1}(z) \frac{\partial}{\partial z} \sum_{\substack{n' \in \mathbb{N} \\ \mathbf{g'}_\| \in \mho_\|}} c_{n'\mathbf{g'}_\|}(z) \left| n'\mathbf{g'}_{\|(z)} \right\rangle \right\}$$
$$+ \frac{2m_0}{\hbar^2} \sum_{\substack{n' \in \mathbb{N} \\ \mathbf{g'}_\| \in \mho_\|}} \left(E - V_{bias}(z) - \varepsilon_{n'\mathbf{g'}_\|}(z) \right) c_{n'\mathbf{g'}_\|}(z) \left| n'\mathbf{g'}_{\|(z)} \right\rangle = 0.$$

Applying the chain-rule for derivatives and multiplying through by $\mathbf{M}(z)$ we isolate the second-derivative of $c_{n'\mathbf{g'}_\|}(z)$. Projecting both sides onto an arbitrary $\left| n\mathbf{g}_\| (z) \right\rangle$, $n \in \mathbb{N}$, $\mathbf{g}_\| \in \mho_\|$, exploiting orthonormality (Eqn. (B.3)) to simplify, and defining,

$$\text{(C.2)} \qquad \mathbf{M}^{[i,j]}(z) \stackrel{\text{def}}{=} \left[\frac{\partial^i}{\partial z^i} \mathbf{M}(z) \right] \left[\frac{\partial^j}{\partial z^j} \mathbf{M}^{-1}(z) \right]$$

we get,

$$\frac{d^2}{dz^2} c_{n\mathbf{g}_\parallel}(z) + \sum_{\substack{n' \in \mathbb{N} \\ \mathbf{g'}_\parallel \in \mho_\parallel}} P^{(\mathrm{BD})}_{n\mathbf{g}_\parallel, n'\mathbf{g'}_\parallel}(z) \frac{d}{dz} c_{n'\mathbf{g'}_\parallel}(z)$$
$$+ \sum_{\substack{n' \in \mathbb{N} \\ \mathbf{g'}_\parallel \in \mho_\parallel}} \left[Q^{(\mathrm{BD})}_{n\mathbf{g}_\parallel, n'\mathbf{g'}_\parallel}(z) + M_{n\mathbf{g}_\parallel, n'\mathbf{g'}_\parallel}(z) K^2_{z,n'\mathbf{g'}_\parallel} \right] c_{n'\mathbf{g'}_\parallel}(z) = 0, \tag{C.3}$$

where

$$\begin{aligned} P^{(\mathrm{BD})}_{n\mathbf{g}_\parallel, n'\mathbf{g'}_\parallel}(z) &= \left\langle n\mathbf{g}_\parallel(z) \right| \mathbf{M}^{[0,1]}(z) + 2\frac{\partial}{\partial z} \left| n'\mathbf{g'}_\parallel(z) \right\rangle \\ &\equiv \iint_{\mathbb{R}^2} \phi^*_{n\mathbf{g}_\parallel}\left(\mathbf{r}_\parallel; z\right) \left[m\left(\mathbf{r}_\parallel, z\right) \left(\frac{\partial}{\partial z} \frac{1}{m\left(\mathbf{r}_\parallel, z\right)} \right) \right] \phi_{n'\mathbf{g'}_\parallel}\left(\mathbf{r}_\parallel; z\right) d^2 r_\parallel \\ &+ 2 \iint_{\mathbb{R}^2} \phi^*_{n\mathbf{g}_\parallel}\left(\mathbf{r}_\parallel; z\right) \frac{\partial}{\partial z} \phi_{n'\mathbf{g'}_\parallel}\left(\mathbf{r}_\parallel; z\right) d^2 r_\parallel, \end{aligned} \tag{C.4}$$

$$\begin{aligned} Q^{(\mathrm{BD})}_{n\mathbf{g}_\parallel, n'\mathbf{g'}_\parallel}(z) &= \left\langle n\mathbf{g}_\parallel(z) \right| \mathbf{M}^{[0,1]}(z) \frac{\partial}{\partial z} + \frac{\partial^2}{\partial z^2} \left| n'\mathbf{g'}_\parallel(z) \right\rangle \\ &\equiv \iint_{\mathbb{R}^2} \phi^*_{n\mathbf{g}_\parallel}\left(\mathbf{r}_\parallel; z\right) \left[m\left(\mathbf{r}_\parallel, z\right) \left(\frac{\partial}{\partial z} \frac{1}{m\left(\mathbf{r}_\parallel, z\right)} \right) \right] \frac{\partial}{\partial z} \phi_{n'\mathbf{g'}_\parallel}\left(\mathbf{r}_\parallel; z\right) d^2 r_\parallel \\ &+ \iint_{\mathbb{R}^2} \phi^*_{n\mathbf{g}_\parallel}\left(\mathbf{r}_\parallel; z\right) \frac{\partial^2}{\partial z^2} \phi_{n'\mathbf{g'}_\parallel}\left(\mathbf{r}_\parallel; z\right) d^2 r_\parallel, \end{aligned} \tag{C.5}$$

$$\begin{aligned} M_{n\mathbf{g}_\parallel, n'\mathbf{g'}_\parallel}(z) &= \left\langle n\mathbf{g}_\parallel(z) \right| \mathbf{M}(z) \left| n'\mathbf{g'}_\parallel(z) \right\rangle \\ &\equiv \iint_{\mathbb{R}^2} \phi^*_{n\mathbf{g}_\parallel}\left(\mathbf{r}_\parallel; z\right) m\left(\mathbf{r}_\parallel; z\right) \phi_{n'\mathbf{g'}_\parallel}\left(\mathbf{r}_\parallel; z\right) d^2 r_\parallel, \end{aligned} \tag{C.6}$$

$$K^2_{z,n\mathbf{g}_\parallel}(z) = \frac{2m_0}{\hbar^2} \left(E - V_{bias}(z) - \varepsilon_{n\mathbf{g}_\parallel}(z) \right). \tag{C.7}$$

Eqn. (C.3) can be expressed in matrix-vector form as Eqn. (4.23) where the matrix $\mathbf{K}^2_z(z)$ is taken to be diagonal with elements calculated according to Eqn. (C.7).

C.2. KE Operator of G. Bastard. Beginning with the substitution of Eqn. (4.18) into Eqn. (4.22), and following the procedure in Sec. C.1, we arrive at Eqn. (C.3) but with $P^{(\mathrm{BD})}_{n\mathbf{g}_\parallel, n'\mathbf{g'}_\parallel}(z) \mapsto P^{(\mathrm{GB})}_{n\mathbf{g}_\parallel, n'\mathbf{g'}_\parallel}(z)$ and $Q^{(\mathrm{BD})}_{n\mathbf{g}_\parallel, n'\mathbf{g'}_\parallel}(z) \mapsto Q^{(\mathrm{GB})}_{n\mathbf{g}_\parallel, n'\mathbf{g'}_\parallel}(z)$, and,

$$P^{(\mathrm{GB})}_{n\mathbf{g}_\parallel, n'\mathbf{g'}_\parallel}(z) \equiv P^{(\mathrm{BD})}_{n\mathbf{g}_\parallel, n'\mathbf{g'}_\parallel}(z) \tag{C.8}$$

$$Q^{(\mathrm{GB})}_{n\mathbf{g}_\parallel, n'\mathbf{g'}_\parallel}(z) = Q^{(\mathrm{BD})}_{n\mathbf{g}_\parallel, n'\mathbf{g'}_\parallel}(z) + \Delta Q^{(\mathrm{GB})}_{n\mathbf{g}_\parallel, n'\mathbf{g'}_\parallel}(z), \tag{C.9}$$

$$\begin{aligned} \Delta Q^{(\mathrm{GB})}_{n\mathbf{g}_\parallel, n'\mathbf{g'}_\parallel}(z) &\stackrel{\mathrm{def}}{=} \left\langle n\mathbf{g}_\parallel \right| \mathbf{M}^{[0,2]} \left| n'\mathbf{g'}_\parallel \right\rangle \\ &\equiv \frac{1}{2} \iint_{\mathbb{R}^2} \phi^*_{n\mathbf{g}_\parallel}\left(\mathbf{r}_\parallel; z\right) \left[m\left(\mathbf{r}_\parallel, z\right) \left(\frac{\partial^2}{\partial z^2} \frac{1}{m\left(\mathbf{r}_\parallel, z\right)} \right) \right] \phi_{n'\mathbf{g'}_\parallel}\left(\mathbf{r}_\parallel; z\right) d^2 r_\parallel. \end{aligned} \tag{C.10}$$

Appendix D. Block-diagonal form of QDL local mode-coupling matrices.

The matrices for all coupling operators in Eqn. (4.23) exhibit definite structure - coupling occurs only between input and output modes that share the same $\mathbf{g}_{\|}$-index. We begin with a general result and exploit this to show that this coupling property holds for special cases.

LEMMA D.1. *Given a fixed $z = z_0$, a function $f(\mathbf{r}_{\|})$ that is periodic with the lateral lattice, and Brillouin zone vectors $\mathbf{g}_{\|}$ and $\mathbf{g'}_{\|}$, the following matrix-element,*

$$
\begin{aligned}
F_{n\mathbf{g}_{\|},n'\mathbf{g'}_{\|}}(z_0) &= \left\langle n\mathbf{g}_{\|}(z_0)\right| f \left| n'\mathbf{g'}_{\|}(z_0)\right\rangle \\
&= \iint_{\mathbb{R}^2} \phi^*_{n\mathbf{g}_{\|}}\left(\mathbf{r}_{\|};z_0\right)\, f\left(\mathbf{r}_{\|}\right)\, \phi_{n'\mathbf{g'}_{\|}}\left(\mathbf{r}_{\|};z_0\right)\, d^2 r_{\|},
\end{aligned} \tag{D.1}
$$

is zero unless $\mathbf{g}_{\|} = \mathbf{g'}_{\|}$, for all $n, n' \in \mathbb{N}$.

Proof. Substituting the Bloch form of the two lateral eigenfunctions from Eqn. (B.1), the integral becomes,

$$
F_{n\mathbf{g}_{\|},n'\mathbf{g'}_{\|}}(z_0) = \frac{1}{(2\pi)^2}\iint_{\mathbb{R}^2} e^{-i\left(\mathbf{g}_{\|}-\mathbf{g'}_{\|}\right)\bullet\mathbf{r}_{\|}} g\left(\mathbf{r}_{\|};z_0\right)\, d^2 r_{\|}, \tag{D.2}
$$

$$
g\left(\mathbf{r}_{\|};z_0\right) \overset{\text{def}}{=} u^*_{n\mathbf{g}_{\|}}\left(\mathbf{r}_{\|};z_0\right)\, f\left(\mathbf{r}_{\|}\right)\, u_{n'\mathbf{g'}_{\|}}\left(\mathbf{r}_{\|};z_0\right). \tag{D.3}
$$

The expression for the integral has become the Fourier transform of $g\left(\mathbf{r}_{\|};z_0\right)$ to the difference between the Brillouin zone vectors. Because $g\left(\mathbf{r}_{\|};z_0\right)$ is periodic with the lateral lattice, we may invoke corollary A.4 to complete the proof.□

PROPOSITION D.2. *The various BZV-subspaces form irreducible invariant-subspaces for the local mode-coupling operators - $\mathbf{P}^{(BD)}(z)$, $\mathbf{Q}^{(BD)}(z)$, $\mathbf{P}^{(GB)}(z)$, $\mathbf{Q}^{(GB)}(z)$, and $\mathbf{M}(z)$ in Eqn. (4.23) - within a QDL.*

Proof. Because the z-derivatives of laterally periodic functions are also laterally periodic, the expressions for the matrix elements of the operators (Eqn. (C.4), Eqn. (C.5), Eqn. (C.8), Eqn. (C.9), Eqn. (C.6) respectively) satisfy the preconditions for invoking the above lemma. From proposition B.1, the lateral eigenbasis is complete and orthonormal. Therefore, each of the above operators maps each basis element to other basis elements within the same BZV-subspace as evidenced by the sparsity in the matrix elements due to the above lemma. Hence the BZV-subspaces are invariant-subspaces for these operators. The matrices for restrictions of these operators to various BZV subspaces are dense for general effective-mass profiles. Hence these subspaces are irreducible. □

The completeness of the lateral eigenbasis leads to the following observation.

COROLLARY D.3. *The intra-slice coupling matrices are the direct sum of their restrictions to all BZV-subspaces, i.e., $\boldsymbol{\mathcal{O}} = \bigoplus_{\mathbf{g}_{\|}\in\mho_{\|}} \boldsymbol{\mathcal{O}}_{\left[\mathbf{g}_{\|}\right]}$, where $\boldsymbol{\mathcal{O}}$ represents operators $\mathbf{P}^{(BD)}(z)$, $\mathbf{Q}^{(BD)}(z)$, $\mathbf{P}^{(GB)}(z)$, $\mathbf{Q}^{(GB)}(z)$, and $\mathbf{M}(z)$.*

COROLLARY D.4. *The matrices for operators $\mathbf{P}^{(BD)}(z)$, $\mathbf{Q}^{(BD)}(z)$, $\mathbf{P}^{(GB)}(z)$, $\mathbf{Q}^{(GB)}(z)$, and $\mathbf{M}(z)$ are block-diagonal in a natural order of the lateral eigenbasis (Def. 4.1).* For $\mathbf{P}(z)$, we get the following expression,

(D.4)
$$\mathbf{P}(z) = \begin{bmatrix} & \ddots & & & & & \\ \cdots & \mathbf{0} & \mathbf{P}_{[\mathbf{g}_\parallel]}(z) & \mathbf{0} & \cdots & & \\ & & & \ddots & & & \\ & & & \cdots & \mathbf{0} & \mathbf{P}_{[\mathbf{g}'_\parallel]}(z) & \mathbf{0}\cdots \\ & & & & & & \ddots \end{bmatrix},$$

where the matrix elements for the operator-restrictions are,

(D.5)
$$P_{[\mathbf{g}_\parallel]nn'}(z) = \left\langle n\mathbf{g}_\parallel \right| \mathbf{M}^{[0,1]} + 2\frac{\partial}{\partial z} \left| n'\mathbf{g}_\parallel \right\rangle.$$

Analogous expressions hold for $\mathbf{Q}(z)$, $\boldsymbol{\Upsilon}^{(i,j)}(z)$, $\mathbf{M}(z)$. The matrix for $\mathbf{K}_z^2(z)$ is diagonal by definition and remains so for any order of basis elements. Hence the whole of Eqn. (4.23) is block-diagonal in a natural order of the basis.

Appendix E. Concise Expressions for Intra-Slice Mode-Coupling Matrix Elements .

Being laterally periodic, the relative-effective-mass lateral profile $m\left(\mathbf{r}_\parallel; z\right)$ and its reciprocal $\mu\left(\mathbf{r}_\parallel; z\right)$ are representable as vectors $\hat{\mathbf{m}}(z)$ and $\hat{\boldsymbol{\mu}}(z)$ of their Fourier-series coefficients as per Section 2.3. Combined with the block-diagonal nature of the intra-slice mode-coupling operators, along with the representation of lateral eigenfunctions in Appendix B, this leads to concise expressions for various matrix elements,

(E.1)
$$M_{[\mathbf{g}_\parallel]n_1n_2}(z) = \hat{\mathbf{u}}^*_{n_1\mathbf{g}_\parallel}(z) \bullet \left(\hat{\mathbf{m}}(z) \odot \hat{\mathbf{u}}_{n_2\mathbf{g}_\parallel}(z)\right),$$

(E.2)
$$P_{[\mathbf{g}_\parallel]n_1,n_2}(z) = \hat{\mathbf{u}}^*_{n_1\mathbf{g}_\parallel}(z) \bullet \left(\hat{\mathbf{m}}(z) \odot \frac{d}{dz}\hat{\boldsymbol{\mu}}(z) \odot \hat{\mathbf{u}}_{n_2\mathbf{g}_\parallel}(z)\right) + 2\Upsilon^{[0,1]}_{[\mathbf{g}_\parallel]\,n_1,n_2}(z),$$

(E.3)
$$Q^{(\mathrm{BD})}_{[\mathbf{g}_\parallel]n_1,n_2}(z) = \hat{\mathbf{u}}^*_{n_1\mathbf{g}_\parallel}(z) \bullet \left(\hat{\mathbf{m}}(z) \odot \frac{d}{dz}\hat{\boldsymbol{\mu}}(z) \odot \frac{\partial}{\partial z}\hat{\mathbf{u}}_{n_2\mathbf{g}_\parallel}(z)\right) + \Upsilon^{[0,2]}_{[\mathbf{g}_\parallel]\,n_1,n_2}(z),$$

(E.4)
$$\Delta Q^{(\mathrm{GB})}_{[\mathbf{g}_\parallel]n_1,n_2}(z) = \hat{\mathbf{u}}^*_{n_1\mathbf{g}_\parallel}(z) \bullet \left(\hat{\mathbf{m}}(z) \odot \frac{d^2}{dz^2}\hat{\boldsymbol{\mu}}(z) \odot \hat{\mathbf{u}}_{n_2\mathbf{g}_\parallel}(z)\right)$$

where

(E.5)
$$\Upsilon^{[i,\,j]}_{[\mathbf{g}_\parallel]\,n_1,n_2}(z) = \frac{d^i}{dz^i}\hat{\mathbf{u}}^*_{n_1\mathbf{g}_\parallel}(z) \bullet \frac{d^j}{dz^j}\hat{\mathbf{u}}_{n_2\mathbf{g}_\parallel}(z).$$

The derivatives of $\hat{\mathbf{u}}_{n\mathbf{g}_\parallel}(z)$ can be calculated numerically by solving the lateral eigenvalue problem of Eqn. (4.19) on a mesh imposed along z, or analytically if appropriate parametric formulae for $m\left(\mathbf{r}_\parallel; z\right)$ and $V_{\mathrm{struct}}\left(\mathbf{r}_\parallel; z\right)$ are used.

The simplified BZV-subspace expression for $\mathbf{G}_0(z)$ in Eqn. (4.31), for both KE operators. From Eqn. (C.4) and Eqn. (C.8), is

(E.6)
$$G^{(\mathrm{BD})}_{0\,[\mathbf{g}_\parallel]\,n_1,n_2} = \frac{1}{2}\hat{\mathbf{u}}^*_{n_1\mathbf{g}_\parallel} \bullet \left(\hat{\mathbf{m}}(z) \odot \frac{d}{dz}\hat{\boldsymbol{\mu}}(z) \odot \frac{d}{dz}\hat{\mathbf{u}}_{n_2\mathbf{g}_\parallel}(z)\right)$$

$$- \frac{1}{2}\frac{d}{dz}\hat{\mathbf{u}}^{*}_{n_1\mathbf{g}_\parallel} \bullet \left(\hat{\mathbf{m}}(z) \odot \frac{d}{dz}\hat{\boldsymbol{\mu}}(z) \odot \hat{\mathbf{u}}_{n_2\mathbf{g}_\parallel}(z)\right)$$
$$- \frac{1}{2}\hat{\mathbf{u}}^{*}_{n_1\mathbf{g}_\parallel} \bullet \left[\left(\frac{d}{dz}\hat{\mathbf{m}}(z) \odot \frac{d}{dz}\hat{\boldsymbol{\mu}}(z)\right) \odot \hat{\mathbf{u}}_{n_2\mathbf{g}_\parallel}(z)\right]$$
$$- \Upsilon^{[1,1]}_{\left[\mathbf{g}_\parallel\right] n_1,n_2}(z) - \frac{1}{4}\left\{\mathbf{P}^2(z)\right\}_{\left[\mathbf{g}_\parallel\right] n_1,n_2},$$

$$G^{(\mathrm{GB})}_{0\left[\mathbf{g}_\parallel\right] n_1,n_2} = G^{(\mathrm{BD})}_{0\left[\mathbf{g}_\parallel\right] n_1,n_2} - \frac{1}{2}\hat{\mathbf{u}}^{*}_{n_1\mathbf{g}_\parallel} \bullet \left(\hat{\mathbf{m}}(z) \odot \frac{d^2}{dz^2}\hat{\boldsymbol{\mu}}(z) \odot \hat{\mathbf{u}}_{n_2\mathbf{g}_\parallel}(z)\right). \tag{E.7}$$

Appendix F. Block-diagonal nature of inter-region mode-coupling matrices .

F.1. Inter-slice coupling in QDL . Substituting the expressions for the wavefunctions from Eqn. (4.37) into Eqn. (5.3) and (5.4) and projecting onto a mode $\left|n_1\mathbf{g}_{\parallel 1}\right\rangle_{j+1}$, Eqn. (5.5) yields, in component-major basis-order,

$$\left\{\boldsymbol{\Theta}_{j+1}\left[\mathbf{a}_{j+1} + \mathbf{b}_{j+1}\right]\right\}_{n_1\mathbf{g}_{\parallel 1}} \delta\left(\mathbf{0}_\parallel\right) = \sum_{n_2\mathbf{g}_{\parallel 2}} x^{(\mathrm{QDL|QDL})}_{1(j+1,\,j)n_1\mathbf{g}_{\parallel 1},n_2\mathbf{g}_{\parallel 2}} \left\{\boldsymbol{\Theta}_j\left[\exp\left(i\boldsymbol{\Xi}_j l_j\right)\mathbf{a}_j + \exp\left(-i\boldsymbol{\Xi}_j l_j\right)\mathbf{b}_j\right]\right\}_{n_2\mathbf{g}_{\parallel 2}}, \tag{F.1}$$

$$\left\{\boldsymbol{\Theta}_{j+1}\boldsymbol{\Xi}_{j+1}\left[\mathbf{a}_{j+1} - \mathbf{b}_{j+1}\right]\right\}_{n_1\mathbf{g}_{\parallel 1}} \delta\left(\mathbf{0}_\parallel\right) = \sum_{n_2\mathbf{g}_{\parallel 2}} x^{(\mathrm{QDL|QDL})}_{2(j+1,\,j)n_1\mathbf{g}_{\parallel 1},n_2\mathbf{g}_{\parallel 2}} \left\{\boldsymbol{\Theta}_j\boldsymbol{\Xi}_j\left[\exp\left(i\boldsymbol{\Xi}_j l_j\right)\mathbf{a}_j - \exp\left(-i\boldsymbol{\Xi}_j l_j\right)\mathbf{b}_j\right]\right\}_{n_2\mathbf{g}_{\parallel 2}}. \tag{F.2}$$

where the expressions for the exchange coefficients are,

$$x^{(\mathrm{QDL|QDL})}_{1(j+1,\,j)n_1\mathbf{g}_{\parallel 1},n_2\mathbf{g}_{\parallel 2}} = \left\langle \left(n_1\mathbf{g}_{\parallel 1}\right)_{j+1} \mid \left(n_2\mathbf{g}_{\parallel 2}\right)_j \right\rangle, \tag{F.3}$$

$$x^{(\mathrm{QDL|QDL})}_{2(j+1,\,j)n_1\mathbf{g}_{\parallel 1},n_2\mathbf{g}_{\parallel 2}} = \left\langle \left(n_1\mathbf{g}_{\parallel 1}\right)_{j+1} \middle| m^{(\mathrm{QDL|QDL})}_{(j+1,\,j)} \middle| \left(n_2\mathbf{g}_{\parallel 2}\right)_j \right\rangle, \tag{F.4}$$

$$m^{(\mathrm{QDL|QDL})}_{(j+1,\,j)}\left(\mathbf{r}_\parallel\right) = \frac{m^{(\mathrm{QDL})}_{j+1}\left(\mathbf{r}_\parallel\right)}{m^{(\mathrm{QDL})}_{j}\left(\mathbf{r}_\parallel\right)}. \tag{F.5}$$

Using the Bloch representation of the eigenfunctions,

$$x^{(\mathrm{QDL|QDL})}_{1(j+1,\,j)n_1\mathbf{g}_{\parallel 1},n_2\mathbf{g}_{\parallel 2}} = \frac{1}{(2\pi)^2}\iint_{\mathbb{R}^2} e^{-i\left(\mathbf{g}_{\parallel 1}-\mathbf{g}_{\parallel 2}\right)\bullet\mathbf{r}_\parallel} \left\{u^{*}_{j+1,\,n_1\mathbf{g}_{\parallel 1}}\left(\mathbf{r}_\parallel\right) u_{j,\,n_2\mathbf{g}_{\parallel 2}}\left(\mathbf{r}_\parallel\right)\right\} d^2r_\parallel, \tag{F.6}$$

$$x^{(\mathrm{QDL|QDL})}_{2(j+1,\,j)n_1\mathbf{g}_{\parallel 1},n_2\mathbf{g}_{\parallel 2}} = \frac{1}{(2\pi)^2}\iint_{\mathbb{R}^2} e^{-i\left(\mathbf{g}_{\parallel 1}-\mathbf{g}_{\parallel 2}\right)\bullet\mathbf{r}_\parallel} \chi^{(\mathrm{QDL|QDL})}_{2(j+1,\,j)n_1\mathbf{g}_{\parallel 1},n_2\mathbf{g}_{\parallel 2}}\left(\mathbf{r}_\parallel\right) d^2r_\parallel, \tag{F.7}$$

$$\chi^{(\mathrm{QDL|QDL})}_{2(j+1,\,j)n_1\mathbf{g}_{\parallel 1},n_2\mathbf{g}_{\parallel 2}}\left(\mathbf{r}_\parallel\right) \stackrel{\mathrm{def}}{=} u^{*}_{j+1,\,n_1\mathbf{g}_{\parallel 1}}\left(\mathbf{r}_\parallel\right) m^{(\mathrm{QDL|QDL})}_{(j+1,\,j)}\left(\mathbf{r}_\parallel\right) u_{j,\,n_2\mathbf{g}_{\parallel 2}}\left(\mathbf{r}_\parallel\right) \tag{F.8}$$

These expressions are Fourier transforms of periodic functions. Corollary A.4 proves that these expressions are identically zero unless $\mathbf{g}_{\parallel 1} = \mathbf{g}_{\parallel 2}$. Therefore, scattering into mode $\left|n_1 \mathbf{g}_\parallel\right\rangle_{j+1}$ takes place only from modes $\left|n_2 \mathbf{g}_\parallel\right\rangle_j$, $n_2 \in \mathbb{N}$. Since $n_1 \in \mathbb{N}$ is arbitrary, all modes $\left|n_2 \mathbf{g}_\parallel\right\rangle_j$ scatter into all modes $\left|n_1 \mathbf{g}_\parallel\right\rangle_{j+1}$ for a given $\mathbf{g}_\parallel \in \mho_\parallel$.

When considering back-scattering, we find that all modes $\left|n_1 \mathbf{g}_\parallel\right\rangle_{j+1}$ scatter into all modes $\left|n_2 \mathbf{g}_\parallel\right\rangle_{j+1}$, $n_1, n_2 \in \mathbb{N}$, for any given $\mathbf{g}_\parallel \in \mho_\parallel$ - the procedure is similar to the above and begins by projecting Eqn. (5.3) and (5.4) onto an arbitrary mode $\left|n_2 \mathbf{g}_{\parallel 2}\right\rangle_j$.

Because $\mathbf{g}_\parallel \in \mho_\parallel$ is arbitrary, we conclude that for each Brillouin-zone vector $\mathbf{g}_\parallel$, scattering occurs only between modes $\left|n_2 \mathbf{g}_\parallel\right\rangle_j$ and $\left|n_1 \mathbf{g}_\parallel\right\rangle_{j+1}$, for all $n_1, n_2 \in \mathbb{N}$. This proves theorem 5.6.

Because of this specific pattern of scattering, the exchange coefficients can be organized into block-diagonal-matrix form in a natural ordering of each eigenbasis in both slices. Observing that all other matrices are also block-diagonal, Eqn. (F.1) and Eqn. (F.2) are concisely expressed in terms of restrictions to an arbitrary BZV-subspace. Considering only non-zero terms in Eqn. (F.1) and Eqn. (F.2), and rearranging to T-matrix form, we get Eqn. (5.11) and Eqn. (5.12).

Concise expressions for the non-zero matrix elements are given in Eqn. (5.13) and Eqn. (5.14).

F.2. Spacer-QDL coupling . For a spacer with region-index j and QDL and region-index $j' = j \pm 1$, we substitute Eqn. (4.8) and Eqn. (4.37) into Eqn. (5.3) and Eqn. (5.4) and get,

$$\text{(F.9)}\quad \sum_{n\in\mathbb{N}} \iint_{\mho_\parallel} \left\{ \boldsymbol{\Theta}_{j'} \left[\begin{array}{c} \exp\left(i\boldsymbol{\Xi}_{j'} z_{j'}\right) \mathbf{a}_{j'}^{(\text{QDL})} \\ +\exp\left(-i\boldsymbol{\Xi}_{j'} z_{j'}\right) \mathbf{b}_{j'}^{(\text{QDL})} \end{array} \right] \right\}_{n\mathbf{g}_\parallel} \phi_{j',n\mathbf{g}_\parallel}\left(\mathbf{r}_\parallel\right) d^2 g_\parallel = \frac{1}{2\pi} \iint_{\mathbb{K}} \left[\begin{array}{c} a_j^{(\text{SPC})}\left(\mathbf{k}_\parallel\right) \operatorname{Ai}\left(\sigma\left(z_j; \mathbf{k}_\parallel, E, V_{0j}, V'\right)\right) \\ +b_j^{(\text{SPC})}\left(\mathbf{k}_\parallel\right) \operatorname{Bi}\left(\sigma\left(z_j; \mathbf{k}_\parallel, E, V_{0j}, V'\right)\right) \end{array} \right] e^{i\mathbf{k}_\parallel \bullet \mathbf{r}_\parallel} d^2 k_\parallel,$$

$$\text{(F.10)}\quad \sum_{n\in\mathbb{N}} \iint_{\mho_\parallel} \left\{ i\boldsymbol{\Theta}_{j'}\boldsymbol{\Xi}_{j'} \left[\begin{array}{c} \exp\left(i\boldsymbol{\Xi}_{j'} z_{j'}\right) \mathbf{a}_{j'}^{(\text{QDL})} \\ -\exp\left(i\boldsymbol{\Xi}_{j'} z_{j'}\right) \mathbf{b}_{j'}^{(\text{QDL})} \end{array} \right] \right\}_{n\mathbf{g}_\parallel} \phi_{j',n\mathbf{g}_\parallel}\left(\mathbf{r}_\parallel\right) d^2 g_\parallel = \frac{1}{2\pi} \iint_{\mathbb{K}} \left[\begin{array}{c} a_j^{(\text{SPC})}\left(\mathbf{k}_\parallel\right) \operatorname{Ai}'\left(\sigma\left(z_j; \mathbf{k}_\parallel, E, V_{0j}, V'\right)\right) \\ +b_j^{(\text{SPC})}\left(\mathbf{k}_\parallel\right) \operatorname{Bi}'\left(\sigma\left(z_j; \mathbf{k}_\parallel, E, V_{0j}, V'\right)\right) \end{array} \right] e^{i\mathbf{k}_\parallel \bullet \mathbf{r}_\parallel} d^2 k_\parallel.$$

It is understood that z_j and $z_{j'}$ are the local z-coordinates for the interface in the respective regions and take the following values depending on the case,

$$\text{(F.11)}\quad \begin{array}{lll} \text{QDL succeeds spacer} \Rightarrow j' = j+1, & z_j = l_j, & z_{j'} = 0, \\ \text{QDL precedes spacer} \Rightarrow j' = j-1, & z_j = 0, & z_{j'} = l_{j'}. \end{array}$$

We now prove theorem 5.8.

Projecting both sides of Eqn. (F.9) and Eqn. (F.10) onto an arbitrary $\left|n\mathbf{g}_\parallel\right\rangle_{j'}$ and rearranging,

$$\sum_{n'\in\mathbb{N}} \iint_{\mho_\parallel} \left\{ \boldsymbol{\Theta}_{j'} \left[\begin{array}{c} \exp\left(i\boldsymbol{\Xi}_{j'} z_{j'}\right) \mathbf{a}_{j'}^{(\text{QDL})} \\ +\exp\left(-i\boldsymbol{\Xi}_{j'} z_{j'}\right) \mathbf{b}_{j'}^{(\text{QDL})} \end{array} \right] \right\}_{n'\mathbf{g}'_\parallel} \delta_{nn'} \delta\left(\mathbf{g}_\parallel - \mathbf{g}'_\parallel\right) d^2 g'_\parallel =$$

$$\iint_{\mathbb{K}_{\|}(E)} x^{(\mathrm{QDL}|\mathrm{SPC})}_{1(j',\,j)n\mathbf{g}_{\|},\mathbf{k}_{\|}} \left[\begin{array}{c} a^{(\mathrm{SPC})}_{j}\left(\mathbf{k}_{\|}\right)\mathrm{Ai}\left(\sigma\left(z_j;\mathbf{k}_{\|},E,V_{0j},V'\right)\right) \\ +b^{(\mathrm{SPC})}_{j}\left(\mathbf{k}_{\|}\right)\mathrm{Bi}\left(\sigma\left(z_j;\mathbf{k}_{\|},E,V_{0j},V'\right)\right) \end{array} \right] d^2k_{\|}. \tag{F.12}$$

$$\sum_{n'\in\mathbb{N}} \iint_{\mho_{\|}} \left\{ i\boldsymbol{\Theta}_{j'}\boldsymbol{\Xi}_{j'} \left[\begin{array}{c} \exp\left(i\boldsymbol{\Xi}_{j'}z_{j'}\right)\mathbf{a}^{(\mathrm{QDL})}_{j'} \\ -\exp\left(i\boldsymbol{\Xi}_{j'}z_{j'}\right)\mathbf{b}^{(\mathrm{QDL})}_{j'} \end{array} \right] \right\}_{n'\mathbf{g'}_{\|}} \delta_{nn'}\delta\left(\mathbf{g}_{\|}-\mathbf{g'}_{\|}\right) d^2g'_{\|} =$$

$$\iint_{\mathbb{K}_{\|}(E)} x^{(\mathrm{QDL}|\mathrm{SPC})}_{2(j',\,j)n\mathbf{g}_{\|},\mathbf{k}_{\|}} \left[\begin{array}{c} a^{(\mathrm{SPC})}_{j}\left(\mathbf{k}_{\|}\right)\mathrm{Ai}'\left(\sigma\left(z_j;\mathbf{k}_{\|},E,V_{0j},V'\right)\right) \\ +b^{(\mathrm{SPC})}_{j}\left(\mathbf{k}_{\|}\right)\mathrm{Bi}'\left(\sigma\left(z_j;\mathbf{k}_{\|},E,V_{0j},V'\right)\right) \end{array} \right] d^2k_{\|}, \tag{F.13}$$

where the expressions for the exchange coefficients are,

$$x^{(\mathrm{QDL}|\mathrm{SPC})}_{1(j',\,j)n\mathbf{g}_{\|},\mathbf{k}_{\|}} = \left\langle \left(n\mathbf{g}_{\|}\right)_{j'} \mid \left(\mathbf{k}_{\|}\right)_{j} \right\rangle, \tag{F.14}$$

$$x^{(\mathrm{QDL}|\mathrm{SPC})}_{2(j',\,j)n\mathbf{g}_{\|},\mathbf{k}_{\|}} = \left\langle \left(n\mathbf{g}_{\|}\right)_{j'} \middle| m^{(\mathrm{QDL}|\mathrm{SPC})}_{(j',\,j)} \middle| \left(\mathbf{k}_{\|}\right)_{j} \right\rangle, \tag{F.15}$$

$$m^{(\mathrm{QDL}|\mathrm{SPC})}_{(j',\,j)}\left(\mathbf{r}_{\|}\right) = \frac{m^{(\mathrm{QDL})}_{j'}\left(\mathbf{r}_{\|}\right)}{m^{(\mathrm{SPC})}_{j}}, \tag{F.16}$$

and $m^{(\mathrm{QDL}|\mathrm{SPC})}_{(j',\,j)}\left(\mathbf{r}_{\|}\right)$ is the ratio-of-effective-mass function for the interface and is periodic. Now, any $\mathbf{k}_{\|}$ can be expressed as the sum of a wavevector within the Brillouin zone and a reciprocal lattice displacement, i.e., $\forall \mathbf{k}_{\|} \in \mathbb{K}, \quad \exists\, \mathbf{q}_{\|} \in \mho_{\|}, (l,m) \in \mathbb{Z}^2 : \mathbf{k}_{\|} = \mathbf{q}_{\|lm} \stackrel{\mathrm{def}}{=} \mathbf{q}_{\|} + \mathbf{G}_{\|lm}$. Then, employing the real-space representations of the states in the above equations (Bloch form for the lateral eigenfunctions from Eqn. (B.1)),

$$\begin{aligned} x^{(\mathrm{QDL}|\mathrm{SPC})}_{1(j',\,j)n\mathbf{g}_{\|},\mathbf{k}_{\|}} &\mapsto x^{(\mathrm{QDL}|\mathrm{SPC})}_{1(j',\,j)n\mathbf{g}_{\|},lm\mathbf{q}_{\|}} \\ &= \mathfrak{F}^{*}_{\|}\left[\phi_{j',n\mathbf{g}_{\|}}\left(\mathbf{r}_{\|}\right)\right]\left(\mathbf{q}_{\|lm}\right) \\ &= \delta\left(\mathbf{g}_{\|}-\mathbf{q}_{\|}\right)\hat{u}^{*}_{j',n\mathbf{g}_{\|},lm}, \end{aligned} \tag{F.17}$$

$$\begin{aligned} x^{(\mathrm{QDL}|\mathrm{SPC})}_{2(j',\,j)n\mathbf{g}_{\|},\mathbf{k}_{\|}} &\mapsto x^{(\mathrm{QDL}|\mathrm{SPC})}_{2(j',\,j)n\mathbf{g}_{\|},lm\mathbf{q}_{\|}} \\ &= \mathfrak{F}^{*}_{\|}\left[m^{(\mathrm{QDL}|\mathrm{SPC})}_{(j',\,j)}\left(\mathbf{r}_{\|}\right)\,\phi_{j',n\mathbf{g}_{\|}}\left(\mathbf{r}_{\|}\right)\right]\left(\mathbf{q}_{\|lm}\right) \\ &= \delta\left(\mathbf{g}_{\|}-\mathbf{q}_{\|}\right)\left(\hat{\mathbf{m}}^{(\mathrm{QDL}|\mathrm{SPC})}_{(j',\,j)}\odot\hat{\mathbf{u}}^{*}_{j',n\mathbf{g}_{\|}}\right)_{lm}, \end{aligned} \tag{F.18}$$

where $\hat{\mathbf{m}}^{(\mathrm{QDL}|\mathrm{SPC})}_{(j',\,j)}$ is the vector of Fourier-series coefficients of the ratio-of-effective-mass function. We have invoked theorem A.3 and corollary A.4 in Appendix A to arrive at the final expressions. The Dirac-delta functions in the above expressions prove that only spacer-region modes $\left|\mathbf{g}_{\|lm}\right\rangle_{j}$ scatter into QDL modes $\left|n\mathbf{g}_{\|}\right\rangle_{j'}$, all $(l,m)\in\mathbb{Z}^2, n\in\mathbb{N}$, and that there is no coupling between modes whose indices differ in the Brillouin-zone vector.

A similar procedure beginning with the projection of both sides of Eqn. (F.9) and Eqn. (F.10) onto an arbitrary $\left|\mathbf{k}_{\|} \stackrel{\mathrm{def}}{=} \mathbf{g}_{\|lm}\right\rangle_{j}$ leads to analogous expressions for back-scattering from QDL modes to spacer modes. The Dirac-delta functions in the expressions for the resulting exchange coefficients, $x^{(\mathrm{QDL}|\mathrm{SPC})}_{1(j,j')lm\mathbf{q}_{\|},n\mathbf{g}_{\|}}$ and $x^{(\mathrm{QDL}|\mathrm{SPC})}_{2(j,j')lm\mathbf{q}_{\|},n\mathbf{g}_{\|}}$, prove that only QDL-region modes $\left|n\mathbf{g}_{\|}\right\rangle_{j'}$ scatter into spacer-region modes $\left|\mathbf{g}_{\|lm}\right\rangle_{j}$ for all $(l,m)\in\mathbb{Z}^2, n\in\mathbb{N}$, and that there is no coupling between modes whose indices differ in the Brillouin-zone vector.

Therefore, forward- as well as backward-scattering between spacer and QDL modes occurs only between modes whose indices share the same Brillouin-zone-vector. This proves theorem 5.8.

The completeness of the set $\mathcal{G}_{[\mathbf{g}_\parallel]} = \left\{ \left| \mathbf{g}_{\parallel lm} \right\rangle_j \mid (l, m) \in \mathbb{Z}^2 \right\}$ in the spacer and the set $\mathbf{\Phi}_{[\mathbf{g}_\parallel]} = \left\{ \left| n\mathbf{g}_\parallel \right\rangle_{j+1} \mid n \in \mathbb{N} \right\}$ in the QDL slice, as basis for $\mathcal{F}_{[\mathbf{g}_\parallel]}$, along with the group-theoretic facts in Appendix A prove corollary 5.9.

Considering only the non-zero terms in Eqn. (F.18) and Eqn. (F.18), applying the relevant case as per Eqn. (F.11), substituting into Eqn. (F.9) and Eqn. (F.10), and manipulating them to arrive at the T-matrix form, we get Eqn. (5.20) and Eqn. (5.26) depending on region-order.

REFERENCES

[1] N. W. Ashcroft and N. D. Mermin, *Solid State Physics*, Brooks Cole, 1976.

[2] G. Bastard, *Superlattice band structure in the envelope-function approximation*, Physical Review B, 24 (1981), pp. 5693–5697.

[3] G. Bastard and J. Brum, *Electronic states in semiconductor heterostructures*, IEEE Journal of Quantum Electronics, 22 (1986), pp. 1625–1644.

[4] G. Bastard, J. K. Furdyna, and J. Mycielski, *Landau levels and cyclotron resonance in graded mixed semiconductors*, Physical Review B, 12 (1975), pp. 4356–4359.

[5] D. BenDaniel and C. Duke, *Space-charge effects on electron tunneling*, Physical Review, 152 (1966), pp. 683–692.

[6] D. Bimberg, M. Grundmann, and N. Ledentsov, *Quantum Dot Heterostructures*, Wiley, 1999.

[7] S. Blanes, F. Casas, J. A. Oteo, and J. Ros, *Magnus and fer expansions for matrix differential equations: the convergence problem*, J. Phys. A: Math. Gen., 31 (1998), pp. 259–268.

[8] J. R. R. Bortoleto, J. G. Zelcovit, H. R. Gutierrez, J. Bettini, and M. A. Cotta, *Designing spatial correlation of quantum dots: towards self-assembled three-dimensional structures*, Nanotechnology, 19 (2008), p. 015601 (8pp).

[9] L. Chang, L. Esaki, and R. Tsu, *Resonant tunneling in semiconductor double barriers*, Applied Physics Letters, 24 (1974), pp. 593–595.

[10] S. Datta, *Electronic Transport in Mesoscopic Systems*, Cambridge Studies in Semiconductor Physics and Microelectronic Engineering, Cambridge University Press, May 1997.

[11] K. Eberl, M. O. Lipinski, Y. M. Manz, W. Winter, N. Y. Jin-Phillip, and O. G. Schmidt, *Self-assembling quantum dots for optoelectronic devices on si and gaas*, Physica E, 9 (2001), pp. 164–174.

[12] L. Goldstein, F. Glas, J. Marzin, M. Charasse, and G. L. Roux, *Growth by molecular beam epitaxy and characterization of inas/gaas strained-layer superlattices*, Applied Physics Letters, 47 (1985), pp. 1099–1101.

[13] B. C. Hall, *Lie Groups, Lie Algebras, and Representations: An Elementary Introduction*, Graduate Texts in Mathematics, Springer-Verlag, New York, 2004.

[14] H. Hasegawa, D. Okada, Y. Horikoshi, and T. Saitoh, *Growth of inas/gaas antidot structure by solid-source mbe*, Japanese Journal of Applied Physics, 41 (2002), pp. 2505–2507.

[15] P. Joyce, T. Krzyzewski, G. Bell, T. Jones, S. Malik, D. Childs, and R. Murray, *Effect of growth rate on the size, composition, and optical properties of InAs/GaAs quantum dots grown by molecular-beam epitaxy*, Physical Review B, 62 (2000), pp. 10891–10895.

[16] C. Kittel, *Quantum Theory of Solids*, Wiley, 2nd ed., Mar. 1987.

[17] D. Y. K. Ko and J. Inkson, *Matrix method for tunneling in heterostructures: Resonant tunneling in multilayer systems*, Physical Review B, 38 (1988), pp. 9945–9951.

[18] E. Kurtz, J. Shen, M. Schmidt, M. Grün, S. Hong, D. Litvinov, D. Gerthsen, T. Oka, T. Yao, and C. Klingshirn, *Formation and properties of self-organized II–VI quantum islands*, Thin Solid Films, 367 (2000), pp. 68–74.

[19] N. N. Ledentsov, V. A. Shchukin, M. Grundmann, N. Kirstaedter, J. Böhrer, O. Schmidt, D. Bimberg, V. M. Ustinov, A. Y. Egorov, A. E. Zhukov, P. S. Kop'ev, S. V. Zaitsev, N. Y. Gordeev, Z. I. Alferov, A. I. Borovkov, A. O. Kosogov, S. S. Ruvimov, P. Werner, U. Gösele, and J. Heydenreich, *Direct formation of vertically coupled quantum dots in stranski-krastanow growth*, Physical Review B, 54 (1996), pp. 8743–8750.

[20] H. Lee, R. Lowe-Webb, W. Yang, and P. C. Sercel, *Determination of the shape of self-organized inas/gaas quantum dots by reflection high energy electron diffraction*, Applied Physics Letters, 72 (1998), pp. 812–814.

[21] S. Y. Lehmann, A. Roshko, R. P. Mirin, and J. E. Bonevich, *Investigation of shape of ingaas/gaas quantum dots*, Materials Research Society Symposium Proceedings, 737 (2003), pp. E13.40.1–E13.40.6.

[22] A. Lenz, H. Eisele, R. Timm, S. K. Becker, R. L. Sellin, U. W. Pohl, D. Bimberg, and M. Dahne, *Nanovoids in ingaas/gaas quantum dots observed by cross-sectional scanning tunneling microscopy*, Applied Physics Letters, 85 (2004), pp. 3848–3850.

[23] D. Leonard, M. Krishnamurthy, C. Reaves, S. Denbaars, and P. Petroff, *Direct formation of quantum-sized dots from uniform coherent islands of InGaAs on GaAs surfaces*, Applied Physics Letters, 63 (1993), p. 3203.

[24] D. Leonard, K. Pond, and P. Petroff, *Critical layer thickness for self-assembled InAs islands on GaAs*, Physical Review B, 50 (1994), pp. 11687–11692.

[25] P. Mazumder, S. Kulkarni, M. Bhattacharya, J. Sun, and G. Haddad, *Digital circuit applications of resonant tunneling diodes*, Proceedings of the IEEE, 86 (1998), pp. 664–686.

[26] E. Merzbacher, *Quantum mechanics*, Wiley, 3rd ed., 1998.

[27] H. Mizuta, C. Goodings, M. Wagner, and S. Ho, *Three-dimensional numerical analysis of multi-mode quantum transport in zero-dimensional resonant tunneling diodes*, Journal of Physics: Condensed Matter, 4 (1992), pp. 8783–8800.

[28] J. Moison, F. Houzay, F. Barthe, L. Leprince, E. André, and O. Vatel, *Self-organized growth of regular nanometer-scale InAs dots on GaAs*, Applied Physics Letters, 64 (1994), p. 196.

[29] Y. Okada, K. Akahane, Y. Iuchi, and M. Kawabe, *Probing the properties of self-organized ingaas quantum dots on gaas (311)b and (001) by conductive atomic force microscope tip*, Materials Research Society Symposium Proceedings, 642 (2001).

[30] H. Saito, K. Nishi, and S. Sugou, *Shape transition of InAs quantum dots by growth at high temperature*, Applied Physics Letters, 74 (1999), p. 1224.

[31] O. Schmidt, U. Denker, K. Eberl, O. Kienzle, F. Ernst, and R. Haug, *Resonant tunneling diodes made up of stacked self-assembled ge/si islands*, Applied Physics Letters, 77 (2000), p. 4341.

[32] R. Shankar, *Principles of Quantum Mechanics*, Springer, 3 ed., Sept. 1994.

[33] G. Springholz, V. Holy, M. Pinczolits, and G. Bauer, *Self-organized growth of three-dimensional quantum-dot crystals with fcc-like stacking and a tunable lattice constant*, Science, 282 (1998), pp. 734–737.

[34] B. Streetman and S. Banerjee, *Solid State Electronics*, Prentice Hall, 6 ed., 2000.

[35] J. Sun, G. Haddad, P. Mazumder, and J. Schulman, *Resonant tunneling diodes: models and properties*, Proceedings of the IEEE, 86 (1998), pp. 641–660.

[36] Z. Wasilewski, S. Fafard, and J. McCaffrey, *Size and shape engineering of vertically stacked self-assembled quantum dots*, Journal of crystal growth, 201-202 (1999), pp. 1131–1135.

[37] H. Xu, *Scattering-matrix method for ballistic electron transport: Theory and an application to quantum antidot arrays*, Physical Review B, 50 (1994), pp. 8469–8478.

[38] M. C. Xu, Y. Temko, T. Suzuki, and K. Jacobi, *Shape transition of self-assembled inas quantum dots on gaas(114)a*, Physical Review B (Condensed Matter and Materials Physics), 71 (2005), p. 075314.

[39] K. Zhang, J. Falta, T. Schmidt, C. Heyn, G. Materlik, and W. Hansen, *Distribution and shape of self-assembled InAs quantum dots grown on GaAs (001)*, Pure and Applied Chemistry, 72 (2000), pp. 199–207.